$7

QEX

May/June 2019

www.arrl.org

A Forum for Communications Experimenters

Issue No. 314

WB9LVI makes a multi-band WSPR transmitter from an Arbitrary Waveform Generator.

ARRL The national association for AMATEUR RADIO™
225 Main Street
Newington, CT USA 06111-1494

KENWOOD

3rd IMDR 110 dB*

RMDR 122 dB*

BDR 150 dB*

Performance Exceeding Expectations.

The most happy and sublime encounters happen in the worst circumstances and under the harshest conditions.

There are enthusiasts who know this all too well because of their love of HF radio.

Results born of certainty and not circumstance. Delivered through impeccable performance. This is our offering to you.

"The Kenwood TS-890S has the highest RMDR of any radio I have ever measured."
- Rob Sherwood - NC0B - December 2018

HF/50MHz TRANSCEIVER

TS-890S

NEW

Top-class receiving performance

3 kinds of dynamic range make for top-class performance.

- Third order intermodulation Dynamic Range (3rd IMDR) 110dB*
- Reciprocal Mixing Dynamic Range (RMDR) 122dB*
- Blocking Dynamic Range (BDR) 150dB*

*Values are measured examples. (2kHz spacing:14.1 MHz, CW, BW 500 Hz, Pre Amp OFF)

- Full Down Conversion RX
- High Carrier to Noise Ratio 1st LO
- H-mode mixer

4 kinds of built-in roofing filters

500Hz / 2.7kHz / 6kHz / 15kHz (270Hz Option)

7 inch Color TFT Display

- Roofing frequency sampling band scope
- Band scope auto-scroll mode
- Multi-information display including filter scope

Clean and tough 100W output

Built-in high-speed automatic antenna tuner

32-bit floating-point DSP for RX / TX and Bandscope

Customer Support: (310) 639-4200

www.kenwood.com/usa

ISO9001 Registered
JVCKENWOOD Corporation

ADS#02119

QEX

May/June 2019

QEX (ISSN: 0886-8093) is published bimonthly in January, March, May, July, September, and November by the American Radio Relay League, 225 Main St., Newington, CT 06111-1494. Periodicals postage paid at Hartford, CT and at additional mailing offices.

POSTMASTER: Send address changes to: QEX, 225 Main St., Newington, CT 06111-1494 Issue No 314

Publisher
American Radio Relay League

Kazimierz "Kai" Siwiak, KE4PT
Editor

Lori Weinberg, KB1EIB
Assistant Editor

Zack Lau, W1VT
Ray Mack, W5IFS
Contributing Editors

Production Department

Steve Ford, WB8IMY
Publications Manager

Michelle Bloom, WB1ENT
Production Supervisor

Sue Fagan, KB1OKW
Graphic Design Supervisor

David Pingree, N1NAS
Senior Technical Illustrator

Brian Washing
Technical Illustrator

Advertising Information Contact:

Janet L. Rocco, W1JLR
Business Services
860-594-0203 – Direct
800-243-7768 – ARRL
860-594-4285 – Fax

Circulation Department

Cathy Stepina, *QEX Circulation*

Offices

225 Main St., Newington, CT 06111-1494 USA
Telephone: 860-594-0200
Fax: 860-594-0259 (24 hour direct line)
e-mail: **qex@arrl.org**

Subscription rate for 6 issues:

In the US: $29;

US by First Class Mail: $40;

International and Canada by Airmail: $35

Members are asked to include their membership control number or a label from their QST when applying.

In order to ensure prompt delivery, we ask that you periodically check the address information on your mailing label. If you find any inaccuracies, please contact the Circulation Department immediately. Thank you for your assistance.

About the Cover

Dr. George R. Steber, WB9LVI, notes that an Arbitrary Waveform Generator (AWG) is an important and flexible instrument available to the experimenter. The AWG Direct Digital Synthesizer technology provides stable, precise, and low distortion signals. With their programmability and arbitrary waveform capability these generators are able to produce a wide variety of complex waveforms specified by the user. A recently available very affordable unit presented the author with an opportunity to use an AWG to create a multi-band WSPR transmitter.

In This Issue

Features

Index of Advertisers

The American Radio Relay League

The American Radio Relay League, Inc, is a noncommercial association of radio amateurs, organized for the promotion of interest in Amateur Radio communication and experimentation, for the establishment of networks to provide communications in the event of disasters or other emergencies, for the advancement of the radio art and of the public welfare, for the representation of the radio amateur in legislative matters, and for the maintenance of fraternalism and a high standard of conduct.

ARRL is an incorporated association without capital stock chartered under the laws of the state of Connecticut, and is an exempt organization under Section 501(c)(3) of the Internal Revenue Code of 1986. Its affairs are governed by a Board of Directors, whose voting members are elected every three years by the general membership. The officers are elected or appointed by the Directors. The League is noncommercial, and no one who could gain financially from the shaping of its affairs is eligible for membership on its Board.

"Of, by, and for the radio amateur," ARRL numbers within its ranks the vast majority of active amateurs in the nation and has a proud history of achievement as the standard-bearer in amateur affairs.

A *bona fide* interest in Amateur Radio is the only essential qualification of membership; an Amateur Radio license is not a prerequisite, although full voting membership is granted only to licensed amateurs in the US.

Membership inquiries and general correspondence should be addressed to the administrative headquarters:

ARRL
225 Main St.
Newington, CT 06111 USA
Telephone: 860-594-0200
FAX: 860-594-0259 (24-hour direct line)

Officers

President: Rick Roderick, K5UR
P.O. Box 1463, Little Rock, AR 72203

Chief Executive Officer: Howard Michel, WB2ITX

The purpose of *QEX* is to:

1) provide a medium for the exchange of ideas and information among Amateur Radio experimenters,

2) document advanced technical work in the Amateur Radio field, and

3) support efforts to advance the state of the Amateur Radio art.

All correspondence concerning *QEX* should be addressed to the American Radio Relay League, 225 Main St., Newington, CT 06111 USA. Envelopes containing manuscripts and letters for publication in *QEX* should be marked Editor, *QEX*.

Both theoretical and practical technical articles are welcomed. Manuscripts should be submitted in word-processor format, if possible. We can redraw any figures as long as their content is clear. Photos should be glossy, color or black-and-white prints of at least the size they are to appear in *QEX* or high-resolution digital images (300 dots per inch or higher at the printed size). Further information for authors can be found on the Web at **www.arrl.org/qex/** or by e-mail to **qex@arrl.org**.

Any opinions expressed in *QEX* are those of the authors, not necessarily those of the Editor or the League. While we strive to ensure all material is technically correct, authors are expected to defend their own assertions. Products mentioned are included for your information only; no endorsement is implied. Readers are cautioned to verify the availability of products before sending money to vendors.

Kazimierz "Kai" Siwiak, KE4PT

Perspectives

QEX Morse Input Design Challenge

Dave "Doc" Evison, W7DE, a new *QEX* subscriber, has issued a challenge to the Amateur Radio community. He writes that he's been licensed since 1954, and that Amateur Radio has been an active part of his long life. Now 86 years old, he's experiencing difficulties with typing skills. He's not alone. Dave writes that many of his daily activities involve keyboarding, and observes that he can send Morse CW faster and with greater ease than he can type. The use of a paddle to input text to a personal computer in Morse format seems like a promising solution to the age-related and disabilities-related keyboard handicap. Since the Amateur Radio community is overflowing with exceptional people with technical skills, resourcefulness, and compassion, a design and construction article by a radio amateur author to remedy this real-life problem seems to be a natural fit.

We agree, and are pleased to implement this as a ***QEX* Morse Input Design Challenge**. The Morse text input device should also implement a small control box, or other method, to be operated with the other hand with keys for Shift, Backspace, Enter, Tab, and so on. The text generated by the Morse input device will require standard keyboard editing for professional formatting and editing. But the Morse input system will work well as a raw text generator for even a professional writer. Morse text input to a personal computer can have significant benefits beyond helping the typing challenged. Finally, use of this device will obviously enhance the operator's Morse code skills, and this will help preserve the legacy and utility of Morse code communications.

The Official Rules

(1) Each entry must appear in the form of a *QEX* construction article that adheres to the *QEX* author's guide and must include:

• Detailed plans (hand drawings are acceptable) and schematics that implement the Morse key input along with a control box or other adjunct implementing Shift, Backspace, Enter, Tab, and other non-Morse characters.

• A list of materials and sources.

• Copy of all software needed to implement the solution.

• Photographs of the completed Morse input solution.

(2) The Morse input device and control box adjunct must be an independent device, not an integral part of another device such as a keyboard or a PC.

(3) Only one entry per individual or team will be accepted. Entrants must be ARRL members. ARRL Headquarters staff and commercial manufacturers, or those associated with commercial manufacturers, are not eligible.

Send your entry article files (photos, text, drawings) to the postal address given below, or via email to **qex@arrl.org** with "*QEX* Morse Input Challenge" and your call sign in the subject line. Do not send zip files as our email system will reject these.

(4) Non-commercial designs only; Morse input devices must be the sole creations of the entrants.

(5) Submission deadline: December 1, 2019.

(6) Judging and prizes: The first five complete articles received (post mark for postal submissions, email time-stamp for electronic submissions), which satisfy all of the listed criteria will be awarded a one-year subscription or extension of your subscription to *QEX*, and will be considered for publication in *QEX*. The decisions of the judges and *QEX* editorial staff are final.

(7) Disclaimer: By participating in the competition, you are verifying that you are the owner and producer of the *QEX* Morse Input Challenge device and its software, and that no third-party ownership rights or patents apply to your design. ARRL acquires no rights to your design, but through your participation you are granting ARRL a perpetual, worldwide, non-exclusive, royalty-free right to publish your entry materials in all media now known or hereinafter created, anywhere in the world, for any lawful purpose.

Writing for *QEX*

Keep the full-length *QEX* articles flowing in, or share a **Technical Note** of several hundred words in length plus a figure or two. Let us know that your submission is intended as a **Note**. *QEX* is edited by Kazimierz "Kai" Siwiak, KE4PT, (**ksiwiak@arrl.org**) and is published bimonthly. *QEX* is a forum for the free exchange of ideas among communications experimenters. The content is driven by you, the reader and prospective author. The subscription rate (6 issues per year) in the United States is $29. First Class delivery in the US is available at an annual rate of $40. For international subscribers, including those in Canada and Mexico, *QEX* can be delivered by airmail for $35 annually. Subscribe today at **www.arrl.org/qex**.

Would you like to write for *QEX*? We pay $50 per published page for articles and Technical Notes. Get more information and an Author Guide at **www.arrl.org/qex-author-guide**. If you prefer postal mail, send a business-size self-addressed, stamped (US postage) envelope to: *QEX* Author Guide, c/o Maty Weinberg, ARRL, 225 Main St, Newington, CT 06111.

Very best regards,

Kazimierz "Kai" Siwiak, KE4PT

Dr. George R. Steber, WB9LVI

11105 N. Riverland Ct., Mequon, WI 53092; **steber@execpc.com**

An Unusual Multi-Band WSPR Transmitter

Use an Arbitrary Waveform Generator to make a multi-band WSPR transmitter.

Arbitrary Waveform Generators (AWG) are among the most important and flexible instruments available to the experimenter. These sophisticated devices employ Direct Digital Synthesizer (DDS) technology to provide stable, precise, low distortion signals. Due to their programmability and arbitrary waveform capability these generators are able to create a wide variety of complex waveforms specified by the user. With these units becoming more affordable, I wondered if an arbitrary waveform generator could be used to make a multi-band WSPR transmitter. Here's how I did it.

WSPR, the "weak signal propagation reporter" digital mode, has always held a special fascination for me. WSPR is able to communicate to the far corners of the world using very little power. A combination of special modulation techniques and software that can reliably decode signals near the noise threshold makes this possible. Joe Taylor, K1JT, and Bruce Walker, W1BW, described the details in their *QST* article[1] "WSPRing Around The World".

Normally, ordinary SSB radio transceivers are used to send and receive WSPR signals using a sound card connection to a PC that is running WSPR software. Actually, you don't always need a transceiver — usually a receiver or transmitter will do. Using just a receiver, teachers, students and short-wave listeners (SWLs) routinely report receptions. They find it instructive and exciting since they can then view real-time results on the *WSPRnet* world map. Receivers work well in this situation because they allow monitoring the entire WSPR band at one time without tuning for individual stations. But Amateur Radio operators usually find that using a transmitter is more fun, which happily provides more targets for the receivers. Sometimes single-band, low-power transmitters[2] are used for this purpose. This takes the strain off the big equipment.

Figure 1 — Photo of FY6600 dual channel function, arbitrary waveform generator used in this project.

AWG Technology

I wondered if AWG technology could be employed to make a stand-alone WSPR transmitter. Modern DDS generators can provide a wide variety of signals. Today's units are capable of sine, square, triangle and numerous other waveforms from 1 μHz to 60 MHz, with variable amplitude and adjustable dc offset. Many generators include features such as variable symmetry, frequency sweep, AM, FM, PM, ASK, FSK and PSK modulation, and gated burst mode, in addition to groups of predefined and user-defined waveforms. The output waveforms are low distortion and available through a nominal 50 Ω output impedance.

Prices of AWGs from the major names have been very high, in some cases more than a thousand dollars. Recently, however, I noticed the price of some lesser known arbitrary waveform generators was falling, making them less costly for general experimentation. While surfing the internet one day, I found a dual channel 60 MHz AWG that seemed to satisfy most of my requirements at the amazing price of US$85 including free shipping. Of particular interest was the 14-bit high speed D/A converter, the 250 MS/s sample rate, and the ability to store 64 arbitrary waveform data files, each one with storage depth of 8192 points and 14 bits. It also supported various standard waveforms

Figure 2 — Photo of WSPR map showing receptions of this unusual transmitter on the 17 meter band.

and modulation types, while functioning as two standard, independent full-function channels, where the phase between channels could be adjusted. Most importantly, the waveform in channel 1 could be modulated by the waveform in channel 2. After another look at the specifications, I placed an order for the FY6600 AWG shown in Figure 1.

Caveat Emptor!

What follows is a description of the trials and tribulations I experienced after discovering several major design deficiencies of the FY6600. I had to perform major circuit board surgery! Details related to making these hardware changes are described in the next section. The sections after that describe the work involved in getting this AWG to transmit a WSPR signal.

In spite of a bad start to this project, it ended happily. Figure 2 shows a *WSPRnet* world map showing the stations that reported receiving my 17- meter signal over a period of about an hour. The remarkable part is that the FY6600 was running just 100 mW into a wire dipole antenna raised just 7 feet above my office floor.

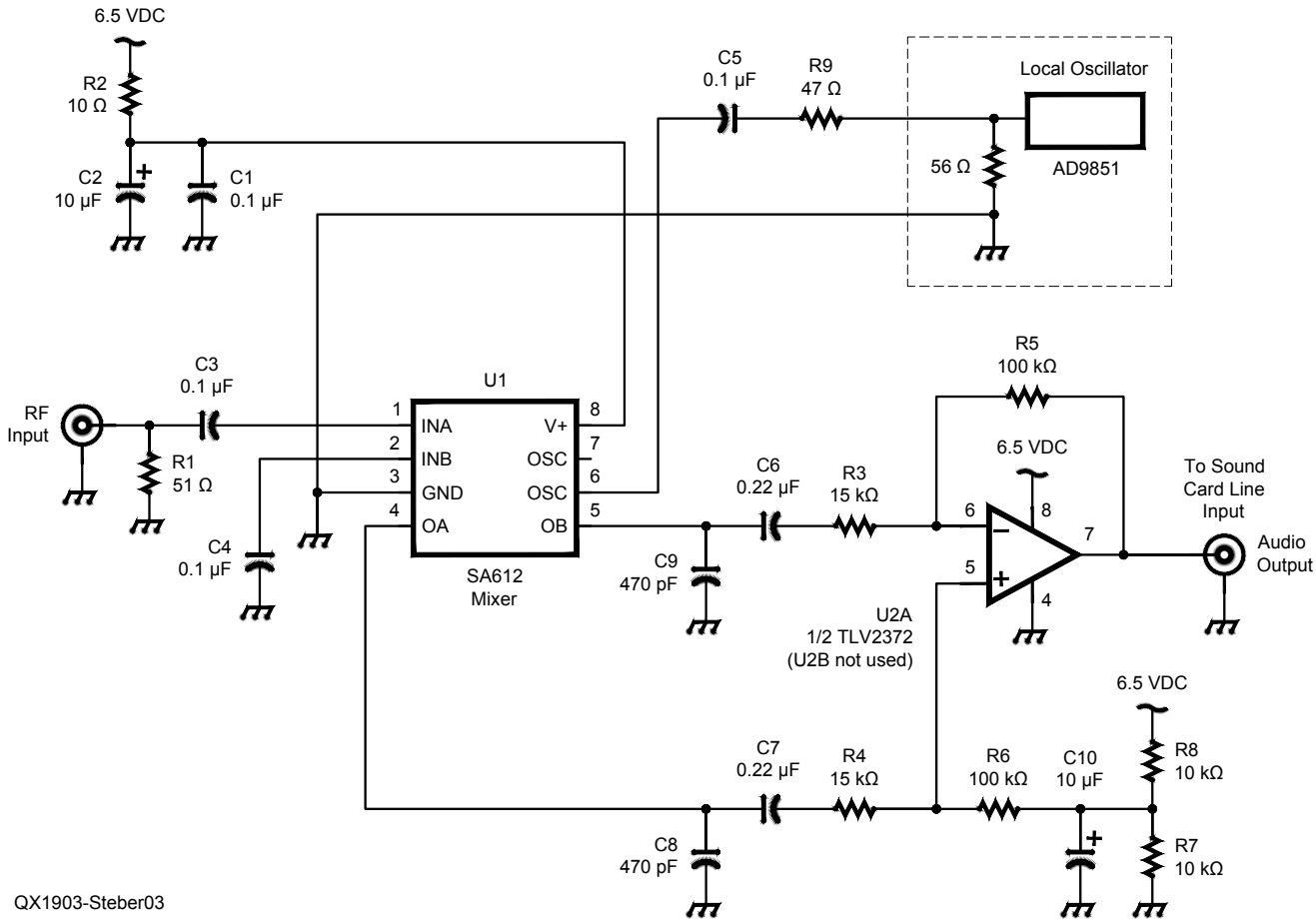

Figure 3 — RF down-converter mixer circuit. Audio output is processed with sound card FFT program. A large FFT is used to look for jitter.

The FY6600 AWG

The 60 MHz FY6600 arrived in good condition several weeks after I placed the order. The number of features it provides is overwhelming. It is a compact dual channel, function generator, arbitrary waveform generator, pulse generator, analog/digital modulator, VCO, sweeper and frequency counter. It has 96 groups of functions and preset waveforms and 64 groups of user-defined waveforms.

It had many features that I wanted to try immediately, such as the variable phase setting between channels, with amazing resolution of 0.01°. I thought this function might be handy for teaching phasor concepts to students. So, right out of the box, I examined this feature using some simple, predictable phase-shift circuits. I used a dual-channel oscilloscope as a phase detector between the two channels. This worked fine and the results agreed well with theory. However, this was not my main reason for obtaining this AWG.

Most of all I wanted to investigate the possibility of modulating the signal of one channel from the other channel. From the user manual, it looked like this would be easy to do. The plan was to generate an RF carrier on channel 1 and modulate it with a baseband WSPR signal from channel 2.

Since WSPR uses very narrow-band 4-FSK modulation, with frequency shift of 1.46 Hz per symbol, it is necessary that the carrier be very stable and not have any significant FM modulation of its own. To check for this possibility, I used a frequency down-converting mixer circuit (Figure 3). This circuit is basically the same as the one described in my *QST* spectrum analyzer article[3]. By choosing a slight offset of the LO frequency from the input signal frequency an audio signal is produced at the output. For this test, the frequency of a 10 MHz RF signal from the AWG is converted to audio and then processed by an FFT program, in this case,[4] *SpectrumView* by Grant Connell,WD6CNF. I used a waterfall plot to look for frequency jitter. Using a large FFT provides high resolution, down to better than1 Hz.

Many low cost DDS signal generators are noted for having more jitter than conventional signal generators. I was not prepared to find the large amount of jitter in the FY6600 signal. Figure 4 shows three sine wave signal generators, operating at about 10 MHz, in an FFT waterfall plot, displaying about 2 FFTs per second. The one in the middle is the FY6600, the one on the left is a Marconi 2022D, and the one on the right is a DDS-based AD9851. The signals on the left and right are shown for comparisons. The FY6600 shows average frequency jitter of 5 to 6 Hz with some peaks up to 10 Hz. There was also significant drift with temperature. My poor WSPR signal would get lost in that amount of noise and drift!

At this point my dreams began to fade for making a WSPR transmitter out of this AWG. I searched the internet for possible answers, and came across the **eevblog.com** forum where problems with the FY6600 were being thrashed out. One of the main problems concerned the stability of the reference 50 MHz oscillator chip used in the design, and the large amount of jitter it contributed to the output signal. Some forum members found that replacing this oscillator chip with a more stable TCXO chip improved stability dramatically. But this involves removing a surface-mount chip and replacing it with another. I was not sure I could do that.

There were other technical problems with this AWG. It seems the designers used a dual output op-amp chip for the signal outputs and that it did not perform well. It had poor frequency response with some distortion at higher frequencies and power levels. Examination of the FY6600 circuit board revealed that it had been originally designed

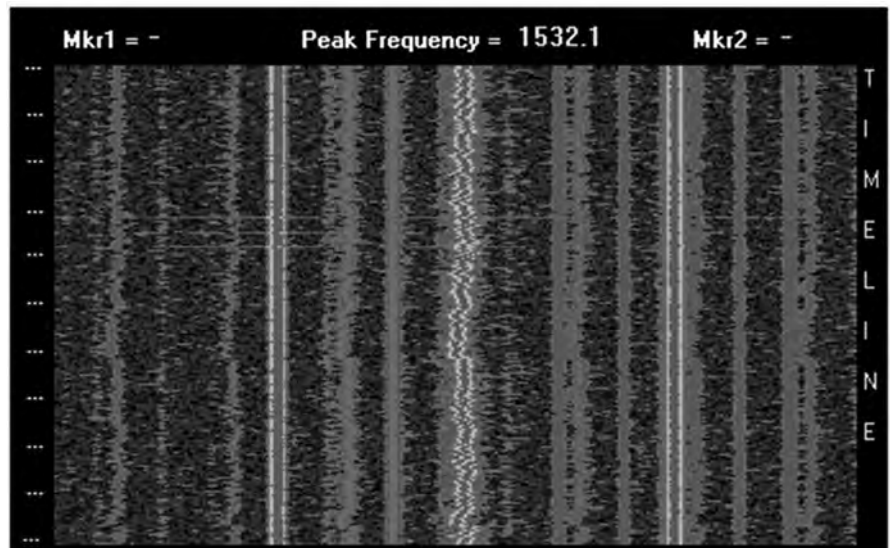

Figure 4 — FFT waterfall plots of three signal generators. The plot in the center is from the FY6600 and has 5 to 6 Hz jitter.

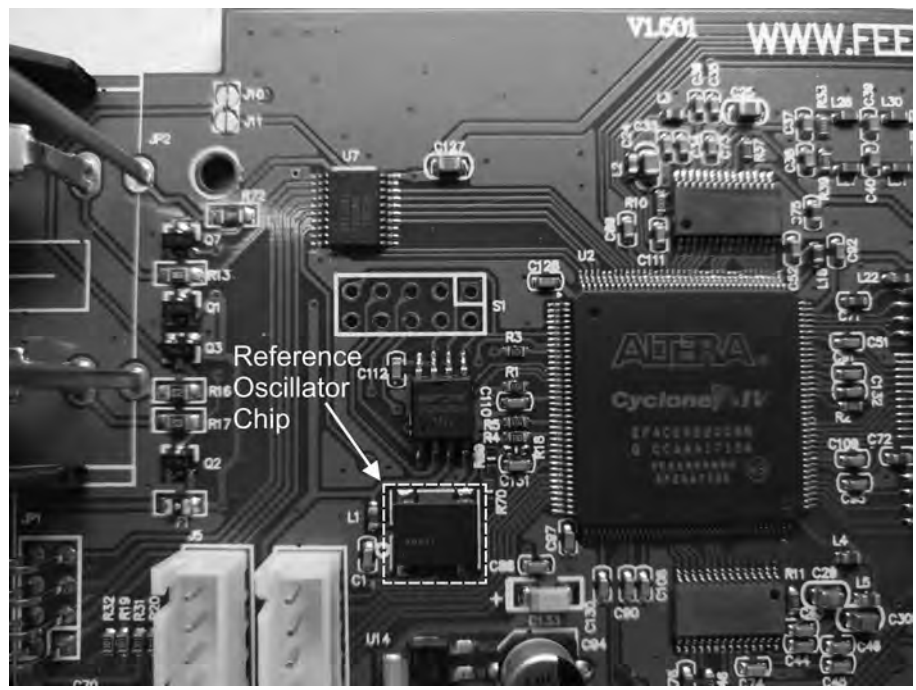

Figure 5 — Photo of main board of FY6600 showing location of the reference oscillator chip.

for separate amplifiers on each channel and the main board was laid out for these chips, but not implemented. Fixing this problem would involve removing another surface mount chip and adding two more chips.

The last problem of importance involved grounding the device to the electrical ac power input. It was inexplicably left floating. This could be remedied by replacing the two-wire ac connector on the back with a three wire grounded ac connector. At last, this was something that could be fixed easily within my capabilities.

After some time for consideration and encouragement from the group at **eevblog.com**, I decided to risk it and go ahead with these three modifications. They are discussed in more detail in the next section.

Modifying the FY6600 AWG

First on the list was to order the parts for the modifications. The three-wire ac connector was already on hand, left over from another project. So I just needed to order the three ICs. I chose to replace my 50 MHz oscillator chip with a Connor Winfield D75J-050.0M TCXO, which has frequency stability of 1 ppm and a nominal 0.5 ps jitter. The two IC op-amps I chose were Texas Instruments THS3095D. They are high-voltage, low distortion, high speed, current-feedback amplifiers available from Digi-Key for US$31.28.

Replacing the Oscillator IC

I replaced the original oscillator chip first. This was the most difficult of the tasks. This IC (Figure 5) is on the main board located close to the lower left corner of the main Cyclone IV processing chip. The forum suggested that a hot air gun be used to remove the IC. I carefully covered the area around the IC with Kapton tape to prevent heat damage to adjacent parts. Then I applied hot air to the IC with a slow circular motion, while at the same time prying the chip with a small tool. After about one minute, the oscillator chip went flying into the air, now free from the board. Fortunately there was no damage to the board pads.

Installing the new 5 mm by 7 mm surface-mount TXCO IC chip was not easy. First of all, the pads on the board were not the same size as the ones on the new IC chip. Another problem was that the new IC did not have any legs that could be used as solder attachments. My solution was to make my own wire legs for the IC. I did this using very flexible silver wire-wrap wire soldered on the tiny pads on the bottom of the IC. With the four legs now soldered to the oscillator IC, I carefully positioned it over the correct pads on the board and soldered pin 1 to the pad. I soldered the other three wire legs in a similar way while holding the legs with needle nose pliers. The final result did not look pretty, but it was solid and proved to work well.

Replacing the Op-amp

Replacing the dual output op-amp was a bit easier. It was located under the main heat sink. I again used a hot air gun to remove this chip. Figure 6 shows where the old op-amp was removed and two new THS3095D ICs were soldered in place. These ICs had legs so they could be soldered in with a fine-tip soldering iron. After installation, I placed the thermal heat pads on top of the new ICs and replace the heat sink.

The Three-wire AC Connector

Installing the new three-wire ac connector on the back was straight-forward but required a lot of filing to enlarge the opening. The back part of the cabinet is very thin so there was a danger of cracking the case. After installing the new connector, I soldered a wire from the ground pin on the connector to the ground plane on the internal power supply. This ensured that the BNC connectors on the front panel were grounded.

Testing the FY6600 AWG Modifications

After I put the FY6600 back together, it was time to see if the modifications worked. First, I tested the reference 50 MHz oscillator, albeit indirectly. A 10 MHz sine wave signal was output on both channels and observed with an oscilloscope. It appeared very clean and noise free.

I examined the 10 MHz signal for jitter using the circuit described above (Figure 3). I found that no jitter could be seen within the limit of my measuring setup — estimated to be 0.1 Hz. The TXCO was stable within about one minute of power on. I saw no perceptible drift in frequency after the short warm-up.

I calibrated the FY6600 in frequency using the procedure found on the forum, since the procedure was not in the manual. I uses a GPS disciplined HP5384A frequency counter for this procedure. After calibration, the AWG was spot on frequency (compared to the LCD displayed value) over most of the range, while deviating slightly, within 2 Hz, beyond 30 MHz. The replacement of the old reference oscillator chip with the new one was hugely successful in solving the major problems of jitter and temperature drift with this AWG.

The new THS3095D output amplifiers performed better than the original dual amplifier. The THS3095D is a high voltage, low distortion, high speed, current-feedback amplifier designed to operate up to ±15 V for applications requiring large, linear output signals. The specification sheet claims a total harmonic distortion as low as -69 dBc at 10 MHz. Observations with a spectrum analyzer confirmed very low levels of distortion. Harmonic distortion was about -69 dBc at 1 MHz, increasing to -38 dBc at 40 MHz, while producing 10 V p-p output into 50 Ω. With this modification, the AWG now provides a nice, clean low-power WSPR signal without the need for filtering.

Implementing the WSPR Transmitter.

With a well-functioning AWG now at

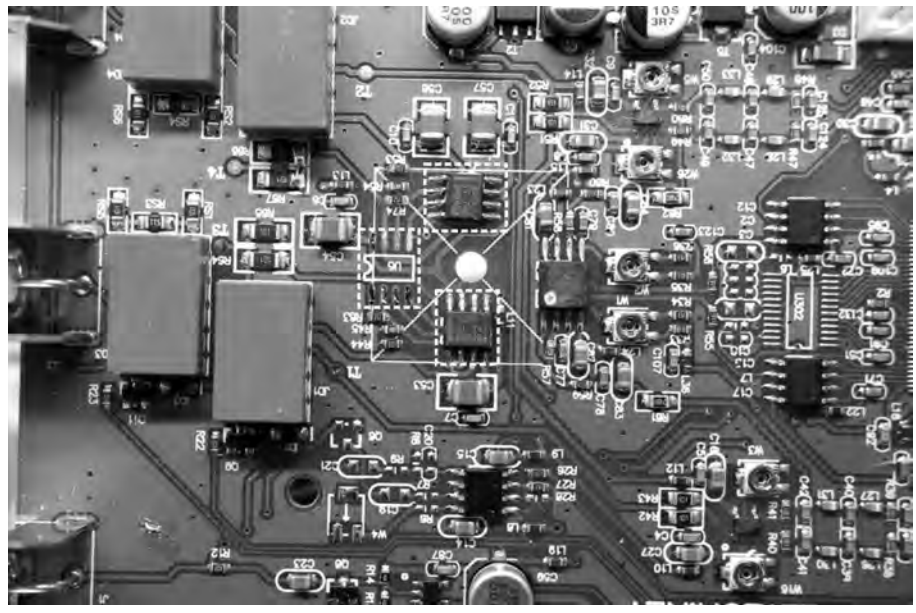

Figure 6 — Photo of main board of FY6600 showing location of the two new amplifier chips near the center of the board. The space to the left of these chips is where the original amplifier chip was located.

hand it was time to consider implementing a WSPR transmitter. The plan was to generate a sine wave RF carrier on channel 1 (CH1) and modulate it with a baseband WSPR signal from channel 2 (CH2). The output of CH1 could then be fed directly from the BNC connector on the front panel to an antenna for transmission. The WSPR band/frequency chosen corresponds to the carrier frequency set in CH1. Hence multi-band WSPR capability is obtained directly.

This particular AWG offers modulation of a carrier on CH1 from either the internal source (from CH2) or via the external VCO input port. It seemed that internal FM modulation of CH1 from CH2 would be the simplest to use. It is effortless to setup. All that is necessary is to click the modulation button and then select FM internal from CH2. The next step is to create a baseband WSPR signal for use in CH2. These details are shown below.

Details of the WSPR Coding

It is helpful to recall some characteristics of a WSPR signal. WSPR modulation is basically continuous phase 4-FSK, with tone separation of 1.4648 Hz. This narrow-band signal occupies a bandwidth of about 6 Hz. Since a transmission can last more than 110 s, frequency stability is a major factor to consider in a WSPR transmitter.

Standard messages are most often used in WSPR communication, and are quite short. They include just a call sign, a 4-digit Maidenhead locator, and the power used in dBm. An example would be "K1ABC FN20 37". There are provisions for compound call signs and/or a 6-digit locator, but these are not discussed further here.

Standard message components after lossless compression are: 28 bits for the call sign, 15 bits for the locator, and 7 bits for the power level, for a total of 50 bits. Forward error correction (FEC) uses another 112 bits. Thus there are a total of 162 bits in each WSPR transmission. The WSPR software on the PC takes the standard message components and creates the 162 binary channel symbols. These symbols are then used to produce the 4-FSK sound output on the PC. In our case we need to take a different route since we are not using a sound card.

We need to find the 162 channel symbols and form a baseband signal equivalent to the 4-FSK tones. Fortunately there are WSPR symbol generator utilities that can create the symbols. One of the easiest to use is[5] *WSPRMSG.exe* by E. C. Marcus, W3PM. It prompts for all inputs and produces a text message with the symbol data.

Table 1 shows the symbol data for my call, location and power, in this case 1 W.

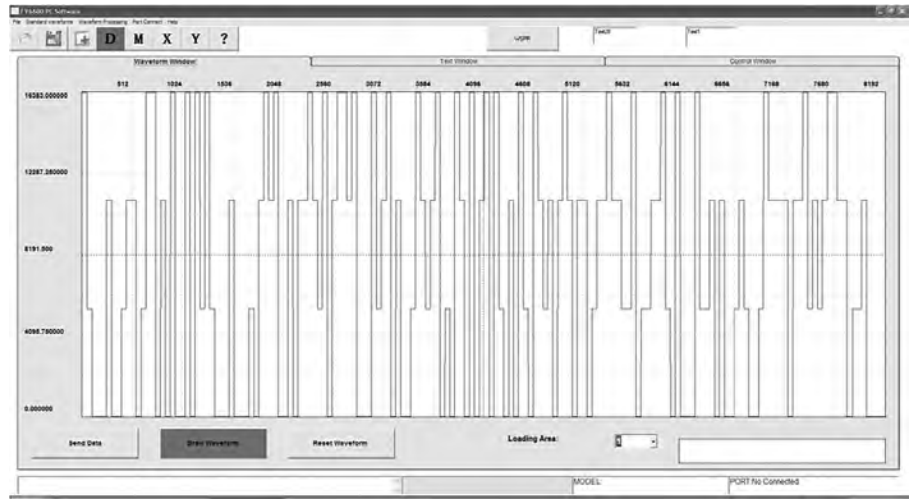

Figure 7 — Screen shot showing the baseband WSPR signal. This waveform is used to FM modulate the sine wave in channel 1.

Table 1.

Symbols for 'WB9LVI EN63 30' (generated from *WSPRMSG.exe*)

3,1,0,0,0,2,0,0,1,2,2,0,1,3,3,0,2,0,3,0,0,3,0,3,1,3,1,0,0,0,2,0,
0,0,1,0,2,3,2,3,0,0,2,0,2,2,3,2,1,3,0,2,3,3,2,3,0,0,0,3,1,2,3,0,
2,0,0,1,3,2,1,2,3,0,1,0,3,2,0,3,0,2,3,0,3,1,0,2,0,3,1,0,3,2,1,2,
0,2,3,2,0,2,2,0,1,2,2,3,2,2,1,1,3,0,1,1,2,2,3,1,0,3,0,0,0,3,1,1,
2,0,2,0,0,1,2,1,0,0,1,3,2,2,2,2,0,2,2,3,1,2,1,2,3,3,2,2,0,1,1,2,
0,0.

Table 2.

WSPR tone frequencies for the Symbols that FSK-modulate the carrier frequency.

Symbol	*tone freq., Hz*
0	0.0 Hz
1	1.4648 Hz
2	2.9296 Hz
3	4.3944 Hz

These 162 symbols comprise my WSPR transmission. Each symbol level changes by 1.4648 Hz. For example, the symbols 0, 1, 2, and 3 correspond to the tone frequencies in Table 2. Each symbol lasts for 683 ms. Hence, the transmission time equals 162 symbols times 0.683 s or 110.646 s. This symbol stream must now be translated and transferred to one of the 64 arbitrary waveform memories of the FY6600 AWG.

The FY6600 has a USB port and the supplied software allows loading of arbitrary waveforms as well as control over the unit. An arbitrary waveform consists of 8192 points with each point having an amplitude in the range of 0 to 16383. Mapping the 'symbol' amplitudes is easy. Let '0' = 0, '1' = 5461, '2' = 10922, and '3' = 16383.

If we use a length of 50 points for each symbol, this uses 8100 points with 92 left over. The left-over points will be at the end of the transmission and ignored. The 8100 points should take 110.646 s, or 73.2 points per second. But since we need to set the period for the entire waveform, including the extra 92 points, we set the period to 111.9 s. This corresponds to a frequency of 0.00893655 Hz set in CH2. But the FY6600 does not have quite that amount of precision and rounds it off to 0.008937 Hz, which yields a period of 111.8943 s, a small difference.

The WSPR waveform is most easily constructed using a spreadsheet. All 8192 points, as defined above, must be entered. Cutting and pasting helps a lot. It is a time-consuming effort, but fortunately has to be done just once. The CSV spreadsheet with the WSPR waveform is then read into one of the waveform memories of the FY6600 where it is saved. Figure 7 shows the resulting waveform as displayed using the FY6600 software. This is the actual FM modulation function that will be applied to channel 1.

WSPR Operation

Operating the AWG as a WSPR transmitter is easy. First select the desired WSPR frequency in CH1 and set it to a sine wave. Then select the baseband WSPR

signal in CH2 from the stored arbitrary waveforms. Set its frequency to 0.008937 Hz. Then select MODE as FM (internal from CH2). Lastly, select the BIAS parameter to 4.5. This parameter tells the unit to use a maximum of 4.5 Hz for the FM modulation. The exact amount will be determined by the FY6600 as the CH2 waveform is played back. These settings can be saved in the AWG for later retrieval.

Now connect your dipole antenna (50 Ω nominal) to the CH 1 output BNC connector. Set the output level to the value desired, typically 2.2 V rms for 100 mW output. You can control the FY6600 from the front panel or by using the PC software via USB.

Start with both CH1 and CH2 off. You need to observe an accurate clock since WSPR transmits on even numbered minutes (0, 2, 4, etc.). The clock must be accurate within 1-2 s of UTC. When the next even minute approaches, just click on CH1 followed by CH2. Your WSPR transmission has just started. At the end of the two minute period, turn off both channels.

This procedure is fine for checking out the unit, and does work well. But it would be nicer if it was automated. Fortunately the FY6600 interface source code in Visual Basic (VB) is provided on the CD. It can easily be modified to automate the process. I created a WSPR button in VB and added it to my software. Now a single click does it. It transmits as two minutes on and two minutes off, continuously. A copy of this code is available on the **www.arrl.org/*QEX*files** web page.

You don't have to be connected to the internet to transmit with WSPR. But to see if you are being received you must check **WSPRnet.org**, enter your call sign and view the map like one shown in Figure 2.

Final Thoughts

This project started out badly when I discovered that the FY6600 had a number of design flaws. Instead of giving up, I employed some difficult surface-mount soldering to salvage the unit. Things worked out well but I cannot recommend this route if you are not well versed in working with these very small chips.

In spite of the difficulties that I encountered, it was very enjoyable to get this multi-band WSPR transmitter on the air. It has provided many hours of enjoyment, and it is very convenient to use. I have employed dipole antennas with a 1:1 current balun with this setup without problems. Dipole impedance varies a bit with height and the proximity to objects, but I did not notice any matching problems. The antennas were resonated in the center of the WSPR band to get the most out of this little transmitter.

Recently I added a 1 W linear amplifier to the output of the AWG. This adjunct has increased the number of receptions by WSPR receivers substantially. So far, I used this transmitter on the 30-, 20- and 17-meter WSPR bands. I must say that the 17 meter band can be full of surprises, as Figure 2 illustrates. One day it is dead and another day full of life.

I hope you enjoyed reading about this WSPR transmitter project. Hopefully it has generated some interest in WSPR. As the technology continues to evolve I expect to see many other innovations. With agreeable propagation, perhaps your WSPR signal will be copied in the far distant regions of the world!

*George R. Steber, PhD, WB9LVI, has an Advanced Class license, is a life member of ARRL and IEEE, and is a Professional Engineer. George is Emeritus Professor of Electrical Engineering and Computer Science at the University Of Wisconsin-Milwaukee. He is now semi-retired, having served over 35 years. His last article for QEX was "A Tunable RF Preamplifier Using a Variable Capacitance Diode" in the November 2017 issue. George has worked for NASA and the USAF and still lectures on special topics at the University. He is currently involved in cosmic ray research and is developing methods to detect and study them on a global basis. When not dodging protons, pions and muons, he enjoys WSPR/JT9 Amateur Radio, racquetball, astronomy, and jazz. You may reach him at **steber@execpc.com** with "WSPR" in subject line and email mode set to text.*

Notes

[1]J. Taylor, K1JT and B. Walker, W1BW, "WSPRing Around The World", *QST*, Nov., 2010, pp. 30-32.
[2]G. R. Steber, WB9LVI, "An Easy WSPR 30 Meter Transmitter", *QST*, Jan., 2015, pp. 47-50.
[3]G. R. Steber, WB9LVI, "Experimenter's RF Spectrum Analyzer", *QST*, Oct., 2008, pp. 36-40.
[4]*SpectrumView* by G. Connell,WD6CNF, **www.hotamateurprograms.com/Vista%20Installs/SpectrumView.exe**.
[5]*WSPRMSG.exe* by E. C. Marcus, W3PM,. **www.knology.net/~gmarcus/WSPR/WSPRMSG.exe**.

Grant Saviers, KZ1W

8730 250th Ave NE, Redmond, WA 98053; **kz1w@arrl.net**

Broad-banding a 160 m Vertical Antenna

Cover the band in four switchable band segments.

Vertical antennas are by far the most popular and cost effective antennas for Top Band operation. A usual problem is a limited bandwidth for SWR less than 2:1, whether they are coil loaded or shortened "T" or "L" top loaded designs. For my western red cedar supported 160 m #13 AWG Copperweld® insulated wire "T" the 2:1 SWR bandwidth is about 80 kHz. It has eight 125 ft long radials elevated 10 ft at the feed point . The top is at about 87 ft and there are 37 ft of "T" arms on each side. The wire is held off the tree trunk at about 6 ft to minimize coupling and losses. My antenna resonates at 1820 kHz at 25 Ω and is fed with a 50 Ω το 25 Ω transmission line transformer, often also called a balun or choke.

I host multi-single teams for CW, SSB, and RTTY contests and use FT8 for DX (Japan stations are at 1908 kHz), so I wanted to be able to cover most of the band with my vertical antenna. The target was less than 1.5:1 SWR across the band since my amplifier was happier with that maximum. I thought a switched capacitor bank to neutralize the inductive reactance at frequencies above the native 1820 kHz resonance would work. My starting design was a series-switched set of parallel binary-weighted values at the feed point, but a suggestion on the Top Band reflector caused me to consider series-switched equal values.

A little work with *EZNEC* showed that three series connected 4000 pF capacitors, each with a shorting relay, would move the feed point 25 Ω SWR minimum in almost equal 40 kHz upward steps. That is, with the four values of 'short', 4000 pF, 2000 pF, and 1333 pF as series 3, 2, 1 capacitors shorted, and then no relay shorting any of them. My *EZNEC* analysis showed that the SWR was now switchable at a maximum 1.5:1 from 1800 to 1970 kHz. Just the last 20 kHz of the band was above 2:1. See the vector network analyzer (VNA) plot of Figure 1 showing measured SWR curves of the four band segments.

Capacitors

Now the question was which capacitors and relays could handle the RF currents and voltages, and the what relays have sufficient coil-to-contact voltage isolation. I used *EZNEC* to find the voltages and currents at high RF power across the capacitors and relay contacts at 25 Ω. As the mismatch reactance increases so does the voltage across the capacitors. Since they all are the same value – 4000 pF – they act as a capacitive equal voltage divider. Thus the voltage at high RF power (total voltage divided by the number of capacitors) per capacitor is about the same, under 250 V in the matching frequency band regardless of the number in series. Of course, with the capacitors in series, the current is always the same in each capacitor, about 8 A at 1500 W into the 25 Ω antenna.

Silver mica capacitors are the best capacitor choice (lowest ESR) if the current ratings are sufficient. CDE rates their CD/CDV16 series for RF current. The more common CD versions have lower current capability. For example, the CDV16 2000 pF 1000 V capacitor is rated 5.3 A continuous at 2.5 MHz and 85 °C. So two in parallel will handle high power level current at 25 Ω. However, I decided to gamble on some eBay Ukraine surplus "transmitting" 1000 V mica capacitors, which looked beefy enough and had screw tabs for mounting. A quick check with my VNA confirmed ESR below what can be accurately measured with its standard bridge and about the same as CDV units, so I had confidence in their power handling

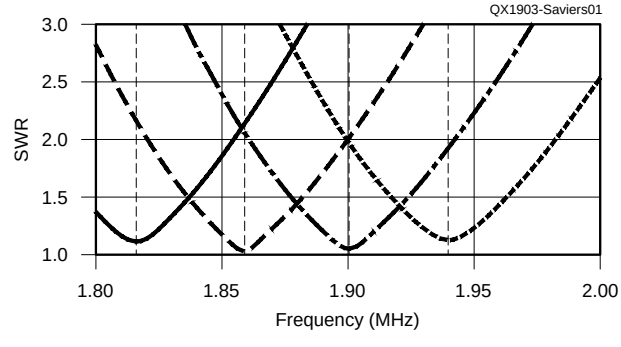

Figure 1 — Measured SWR curves at 1816 kHz, 1859 kHz, 1900 kHz and 1940 kHz center frequencies.

capability. To be extra sure, I paralleled two 2000 pF on standoff spacers for each 4000 pF value. With capacitors in hand the next step was to find a suitable relay.

Relays

My biggest concern was enough coil-to-contact voltage isolation so there was minimal chance of high RF power coming back into the shack via the relay driver wires. In case an operator transmitted outside the frequency range of the selected capacitor value, that could be more than 1000 V. Another consideration was short and direct leads to the relay contacts. I never expected hot switching, so 10 A or better contact ratings seemed sufficient. I found a 12 V dc PCB relay by Schrack (RZ01-1A4-D012) with a plastic arm from the coil armature to the contacts that is rated 5000 V coil to contact isolation, 12 A at 250 V ac switching, and has redundant leads to the Ag/Ni (90/10) contacts through flat alloy copper leads. This was an ideal and inexpensive ($2.59 at Digikey 12/2016) solution. While the 250 V ac load rating is about the maximum expected capacitor voltage, the open contact isolation voltage is 1000 V rms, more than sufficient if not hot switched. Although these relays are not hermetically sealed, the case is sufficiently tight to prevent dirt or insect ingress (Figure 2). Nearly sealed, very small size, very low cost, and an extra-short RF path are all a big plus over open frame relay alternatives. A couple of years of operation at high RF power levels and the usual mistakes of moving outside the tuning range enough to trip the amplifier protection circuits have not caused observed relay damage.

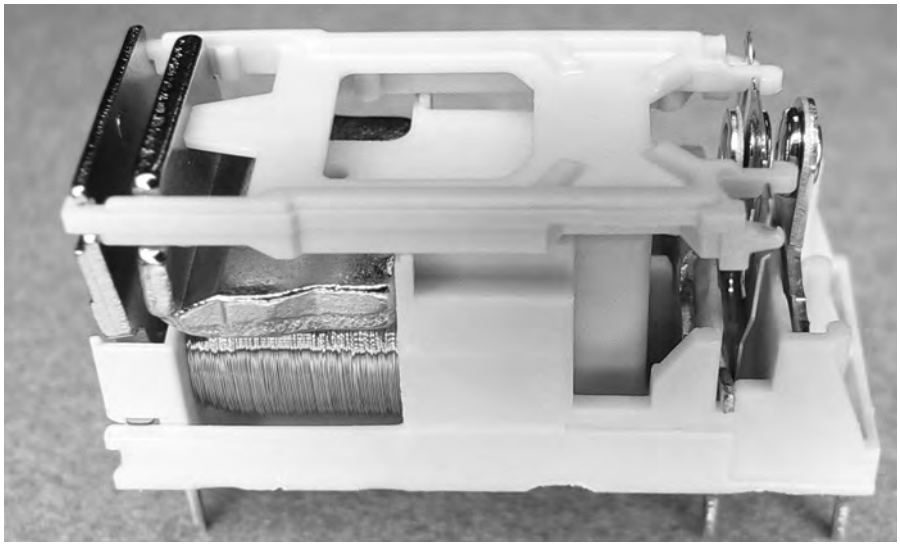

Figure 2 — The Schrack relay.

I added 39 kΩ 2 W Allen Bradley carbon composition resistors across each capacitor to drain and equalize any static charge since all relays are open when power is off. At high RF power the dissipation in any resistor is about 1.5 W at 100% duty cycle. The three capacitors, resistors, and relays were mounted in a 3.5" by 6" by 3" watertight plastic box and connected between the transmission line transformer output and vertical wire (Figure 3). The transformer is a dc short between the vertical wire and radials.

The Control Head

A 4-conductor cable carries the 12 V dc relay signals from the relay box to the shack. The wires are wound through a small ferrite toroid inside the relay box and each relay coil is bypassed with a 0.01 μF ceramic capacitor, see Figure 4 and Figure 5.

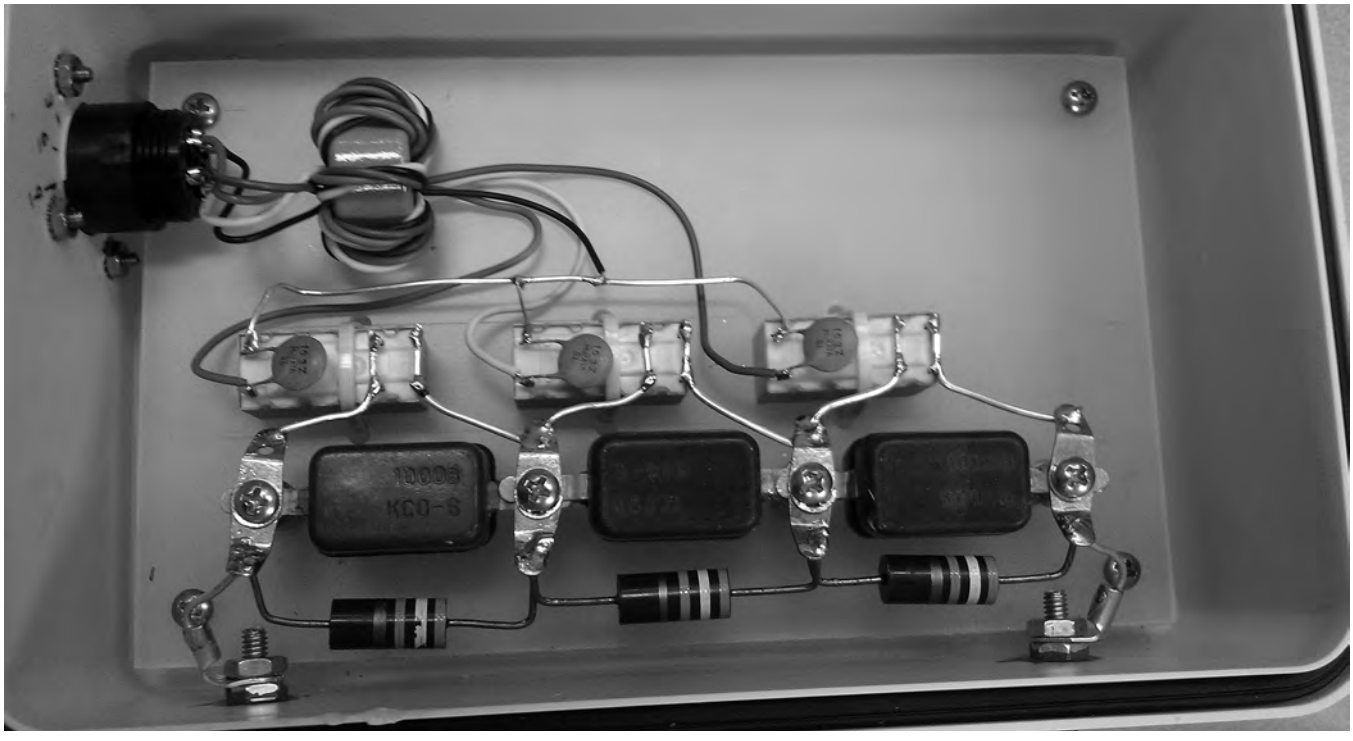

Figure 3 — Inside of the remote switch box after 3 years of operation.

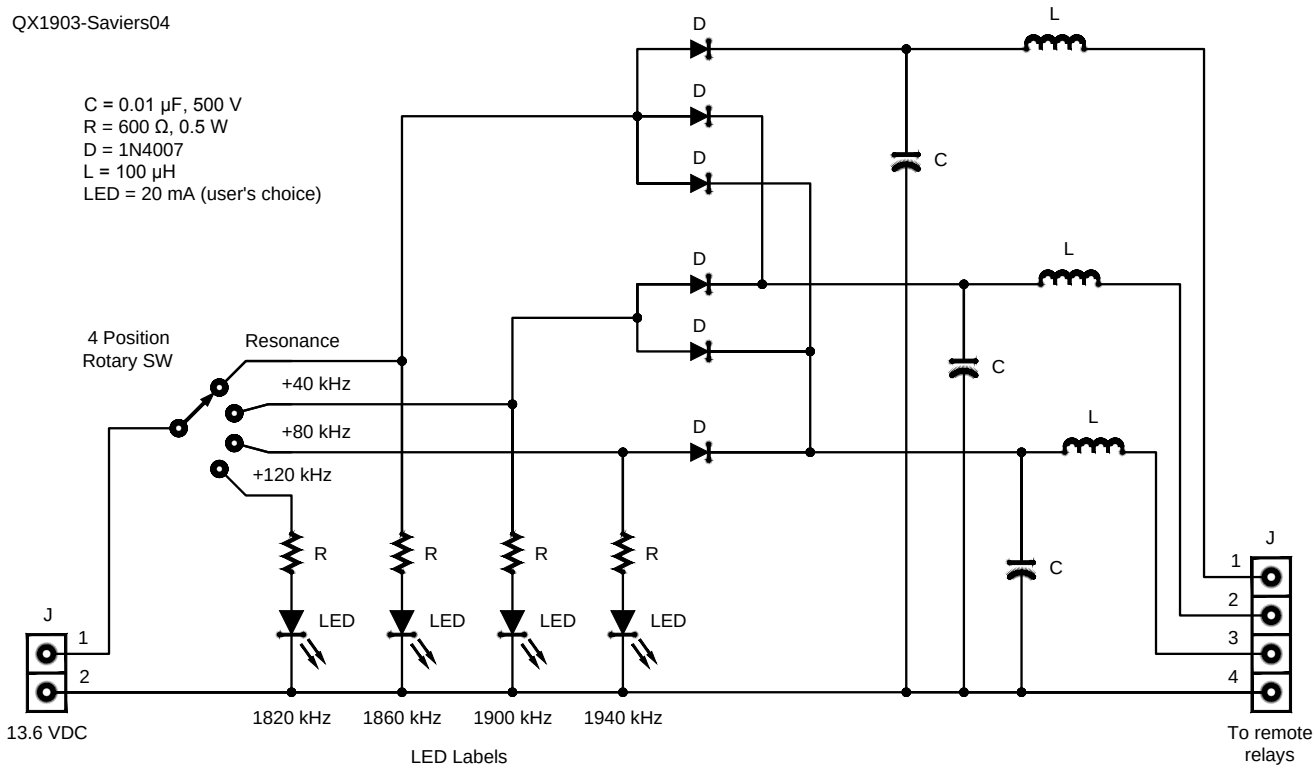

Figure 4 — Schematic of 160 m controller.

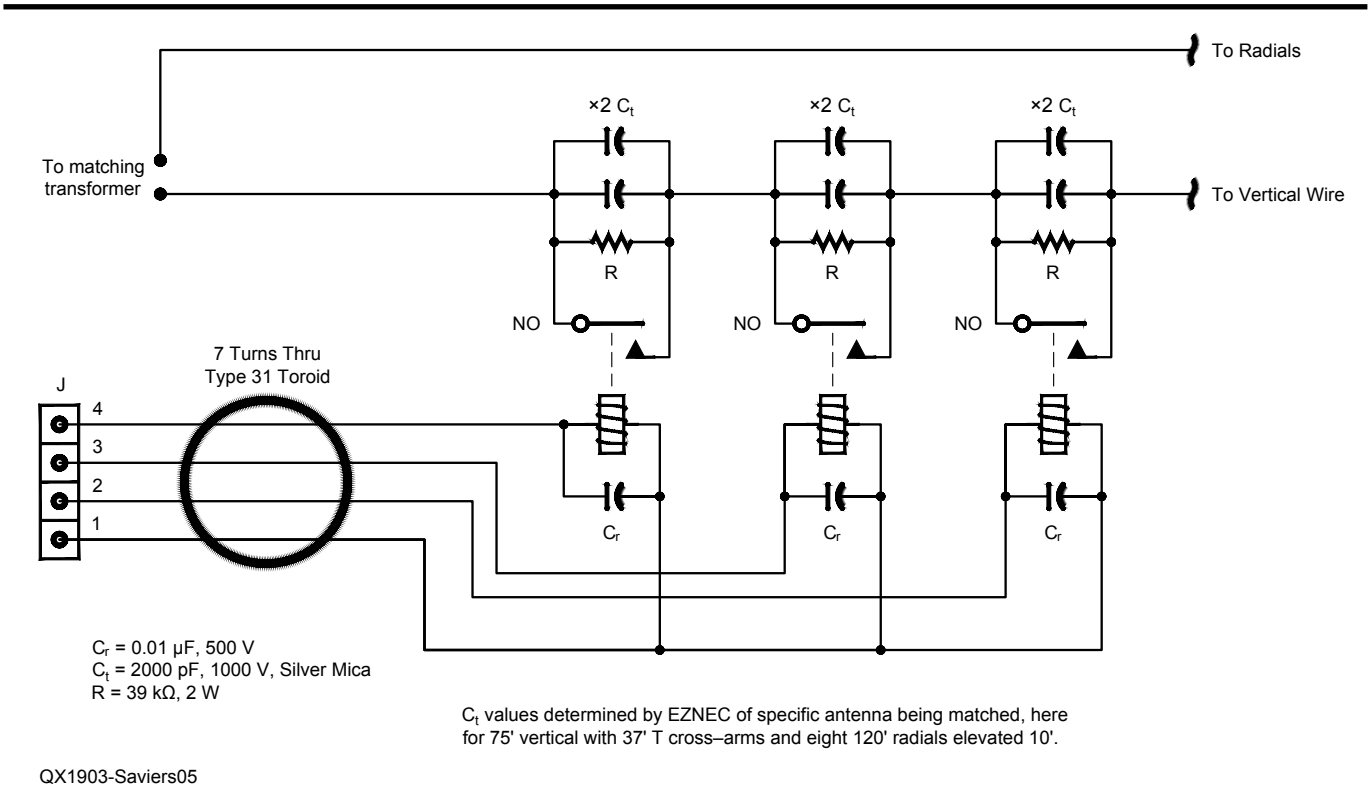

Figure 5 — Schematic of 160 m remote tuner.

For the control head (Figure 6) I use a rotary switch to select, and LEDs to show the selected band segment. It is less error prone than individual SPST toggle switches for each relay. I used a 1N4007 1,000 V 1 A diode tree to select 3, 2, 1, and 'no' relay energized. The combinations of relays to open or close is arbitrary. While 1N1418 diodes would handle the relay voltages and current, I've had them vaporized by surges from nearby lightning strikes. By-pass capacitors and series inductors on each line help keep RF out of the shack 12 V power system, and noise out of the antenna. I designed a simple PCB for the diode tree, but a perf board would work equally well. Figure 7 shows provisions for up to six relays and switches to make all decodes adjustable

The input of the transmission line transformer (Figure 8) uses four type 31 ferrite cores with RG174 TFE coax wound choke, per the designs of K9YC and G3TXQ for 160 m. The RG8 feed coax and 4 conductor control cable are in buried 1.25" PVC conduit, about 120' to the shack entrance.

Conclusions

I have built cage dipoles, and I was very reluctant to consider that design for a broadband vertical supported by a tree in a partially wooded area. Top loading and elevated radials make for more than enough wires to manage. For the radials, I use aluminum electric fencing wire, which has proven very durable, stretch-free, and inexpensive. The #12-1/2 AWG aluminum wire has survived 3" branch drops, 2" of ice, but not a falling 12" caliber tree. It is available in #9 to #17 AWG.

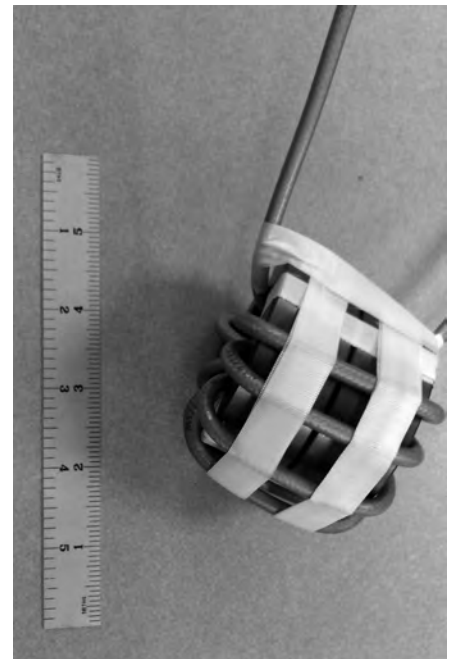

Figure 8 — Feed line choke comprises RG174 TFE coax wound on FT240-31 cores.

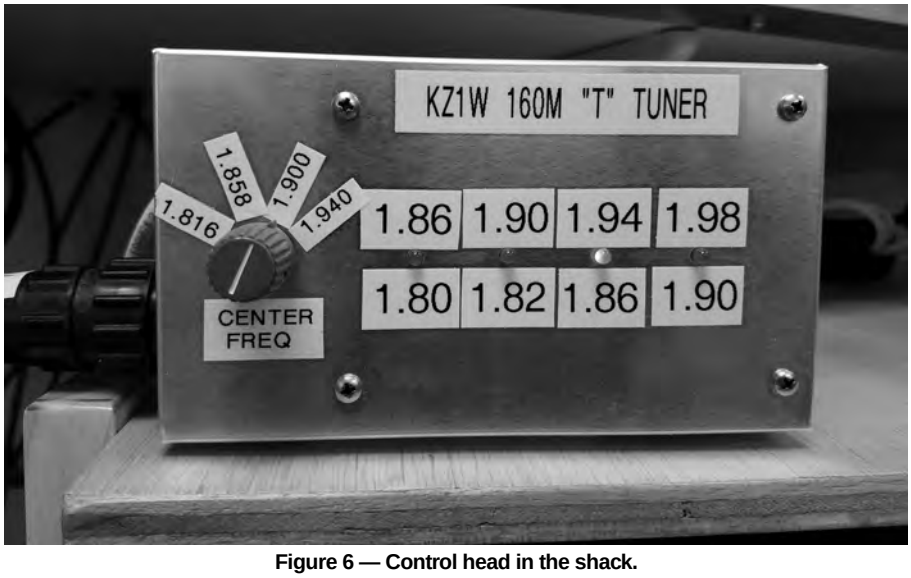

Figure 6 — Control head in the shack.

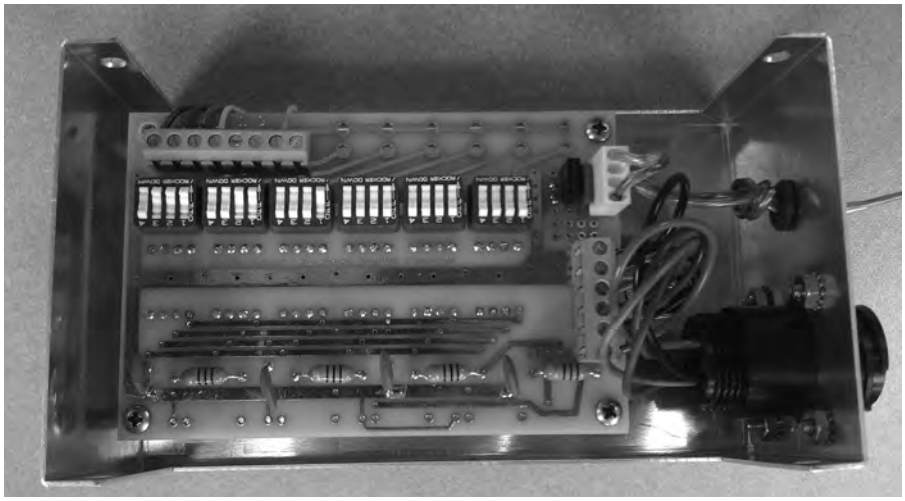

Figure 7 — Provisions for 6 relays and switches to make all decodes adjustable.

Top loading shortened verticals has been shown superior to coil loading in several studies. I am also partial to matching resonant antennas with TLTs since they have very low losses and wide bandwidths. While tuned circuits with variable inductors and capacitors can match over a band, they do so at a higher cost, larger size, longer time to change frequency and greater weather sensitivity. My switched fixed capacitor matcher parts cost was about US$100 for everything, excluding the control cable.

This design is easily modified to broadbanding an 80 m vertical. The capacitor values will be different for different antenna geometries, so an *EZNEC* analysis is a good starting point. It is also possible to automate the segment switching using band decoders with programmable segment frequencies.

My thanks to Rudy Severns, N6LF, for his extensive research about elevated radial systems. See his *QEX* series on this topic.

Grant Saviers, KZ1W, was first licensed K3JEB circa 1958. After receiving a BS and MS degrees in Engineering, he was inactive many years during his career in the computer storage and PC industry. He relicensed as KZ1W in 1982 for offshore sailing communications. His interests are DXpeditoning (E51MKW, TX5D, TX7G, and maritime mobile on cruise ships), modeling and building antennas, and contesting from his Redmond, WA station. He has been chasing DX since 2011 when he started building his current station. Grant also entertains himself in his large hobby machine shop.

Ryan Gedminas, WW6RAG
4734 Ramsay Ave., San Diego, CA 92122; **sirryan2013@gmail.com**

Weather Balloon Hunting

Radiosondes are one-time-use devices that can be tracked, hunted down and recovered. Here's how.

Twice daily the National Weather Service (NWS) launches weather balloons from roughly 90 locations across the United States. The International Observation times are 00:00 Z and 12:00 Z, and so most launches happen one hour earlier. The devices consist of a helium or hydrogen filled balloon. Attached to the balloon with twine is a parachute and a radiosonde.

A radiosonde is a single-use instrument that transmits GPS position, altitude, atmospheric pressure, temperature, and relative humidity as the balloon carries it into the atmosphere. This data is collected in real time during the ascent by a designated monitoring station and used to predict weather and to model wind patterns, as well as provide critical information to aircraft.

Several models of radiosondes are used by weather agencies around the world. The two main manufacturers are Vaisala and Lockheed Martin. In the US the Vaisala RS92-NGP and Lockheed Martin LMS6 are the most popular radiosondes

Radiosonde Launch

I was first introduced to atmospheric instrumentation while reading "RTL-SDR Tutorial: Receiving Weather Balloon (Radiosonde) Data with RTL-SDR".[1] What really ignited my interest was that the radiosondes are not actively recovered after landing. Therefore, if I could process and decode the signal then I might be able to recover one.

The first step of radiosonde hunting was to determine their transmission frequency and packet protocol. Radiosondes around the world typically transmit at 403 MHz. However, my research found that in the United States the NWS often uses 1680 MHz or 1676 MHz in the meteorological band.

There is a map of all the U.S. launch sites on the NWS Upper Air Observations webpage.[2] I contacted the local NWS office and inquired about attending a launch. The earliest tour that they offered was three months away. Impatient, I headed out to the launch site (Figure 1) and arrived at 00:00 Z (5:00 PM local time) but could not see a balloon. Later research revealed

Figure 1 — The radiosonde launch site.

that launches happen 45 minutes before the official observation time. I returned a few days later with a laptop, RTL-SDR, and a 3 dB gain omni directional antenna and began the process of receiving and decoding the signal. Upon launch (Figure 2) I could immediately see the signal, but it took another month of trial and error to find a software configuration that would decode the data that I received.

The Receiver and Antenna

My next challenge was to enhance the performance of my receiving system by filtering and amplifying the signal. I built a proof-of-concept 1680 MHz band-pass filter using a mint tin, a TA1579A SAW filter[3] and two SMA connectors, see Figure 3. For amplification, I used the SPF5189 50 - 4000 MHz low noise amplifier, and provided 5 V dc via a USB cable connected to a portable power pack. Later, NooElec released the SawBird, which is an amplifier and SAW filter combination. I now use their GOES+ version instead of my original filter and amplifier combination.

I evaluated different antenna configurations including an omni-directional ground-plane antenna, and a 14-element Yagi-Uda array intended for the 2.4 GHz Wi-Fi band. Unlike most radiosondes, the RS92-NGP transmits a circularly polarized signal, so I built a helical antenna (Figure 4) using a piece of 2" PVC and circular sheet metal disk along with copper wire. With this antenna, filter, and amplifier the signal was clean and strong for distances of about 64 km. In my current configuration I use an Altelix 2.4 GHz Wi-Fi grid dish antenna. It

Figure 2 — The ascending balloon.

Figure 3 — Prototype filter in a tin housing.

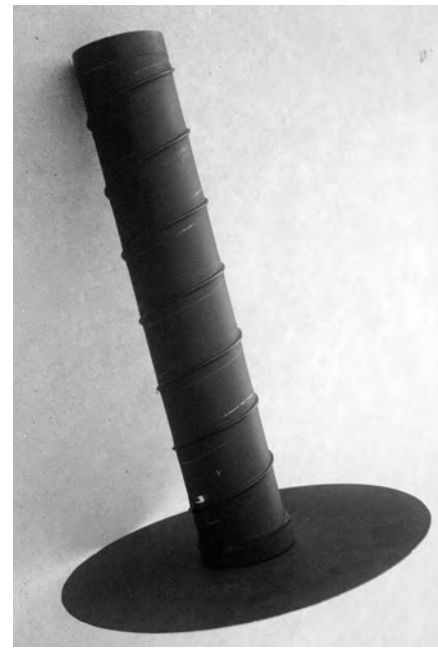

Figure 4 — Home-built helical antenna.

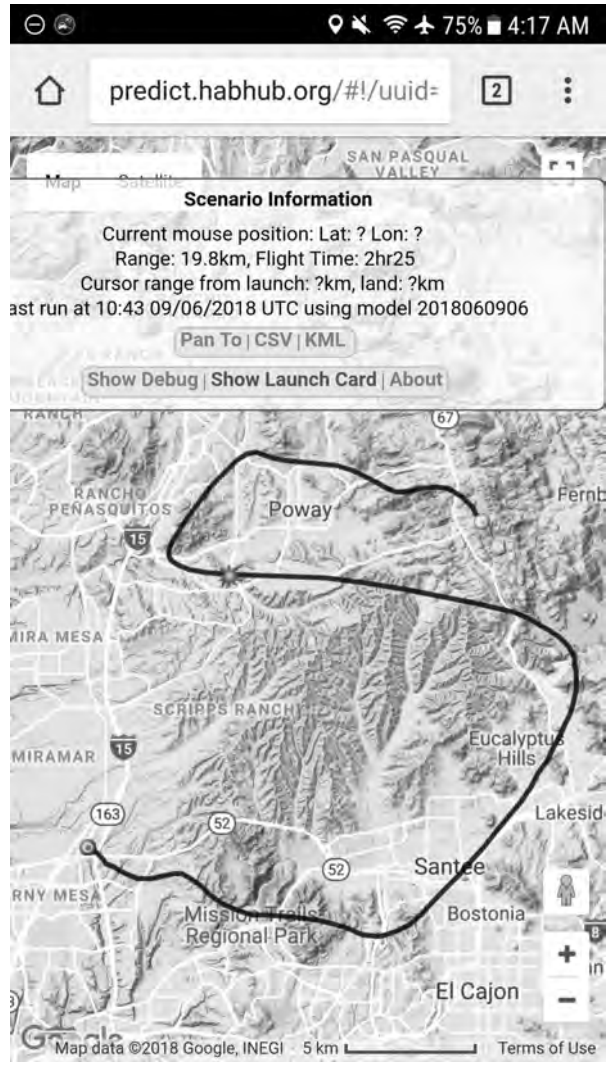

Figure 5 — Predicted radiosonde path.

helps keep a strong signal from the time the radiosonde is launched until it falls below the radio horizon.

Software

I used *SDRSharp* by Airspy to tune my Nooelec NESDR SMArt XTR. I then piped the audio signal using *VB-Audio* into *SondeMonitor* by COAA. Note that *SondeMonitor* produces known errors when calculating location and requires manual operation. *Auto_RX* is designed to run on a single-board computer like a Raspberry Pi. It automatically detects the radiosonde in a user-set search frequency range and begins to decode it, uploading the data to online tracking sites including HabHub Tracker (**habhub.org**).

With this setup, the balloon position could be plotted in real time on a Google Earth map. To get real-time predictions of the landing location, current positions are continuously uploaded to HabHub, which uses position and the NOAA GFS wind models to predict a flight path and the most likely touchdown location. An added benefit of this web page is that others can view the paths and assist in the recovery.

Tracking and Recovery

As I finalized the software and hardware testing, my NWS appointment came, and I was able to attend and assist in an official launch. This afforded me the opportunity to confirm the manufacture and model of the radiosonde and to see what it looked like. I was ready. As hunting day approached, I ran predictions (Figure 5) with **predict.habhub.org** to get an idea of the balloon flight path. From the available data on the morning of the 12:00 Z launch, there would be less wind and therefore less needed driving. At 11:30 Z we drove to a hilltop park where there would be radio line-of-sight to most of the flight path. From there we were able to track the balloon from launch, through balloon burst and two-thirds of the decent, see Figure 6. We positioned ourselves in the nearest parking lot to the predicted landing location, and within three minutes we could see the red parachute drifting down slowly. I walked over and picked it up. After my months of preparation, I was successful on my first attempt, and recovered the radiosonde, see Figure 7.

My special thanks go to Mark Jessop, and Michael Wheeler for their extensive support, and to Jimmy Taeger for the launch-site tour.

Ryan Gedminas, WW6RAG, is a high school student. He earned his Amateur Radio license in June of 2018 while working on this project and pursuing his BSA Eagle Scout rank. Ryan is interested in RF and electrical engineering. He was attracted to Amateur Radio after getting into software defined radio, specifically the RTL-SDR. "What really drew me in was discovering all the information that is beyond sight or sound." Ryans projects twitter@ryan_gedminas

Notes

[1]**https://www.rtl-sdr.com/receiving-weather-balloon-data-with-rtl-sdr/**.
[2]NWS Nashville Upper Air Information; **www.weather.gov/ohx/upperair**.
[3]Saw filter; **https://www.rfmw.com/ProductDetail/TA1579A-TST/466032/**.

Figure 6 — Actual radiosonde flight path [Google Maps].

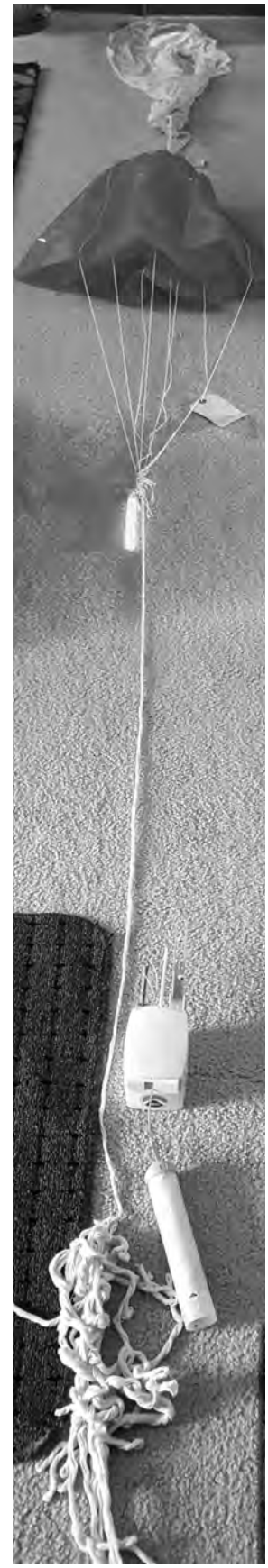

Figure 7 — The recovered radiosonde.

Stefan Scholl, DC9ST
Malvenweg 3, 89160 Dornstadt, Germany; **dc9st@panoradio-sdr.de**

TDOA System for Transmitter Localization

A simple and cheap system for localizing signals in a city uses three or more non-directional receivers at different locations to capture the differences in the arrival time of the signals.

Transmitter localization is both an interesting and challenging task. In addition to applying triangulation in combination with some type of direction finding receivers — using directional antennas, pseudo-Doppler or the interferometer principle — the time-difference-of-arrival (TDOA) method is also widely used. In TDOA three or more non-directional receivers at different locations capture the unknown transmitted signal. Differences in the arrival time of the signals is then used to calculate the transmitter position.

This article provides a short introduction to localization with TDOA. It then presents a simple experimental localization system based on three receivers, each consisting of a RTL-SDR USB-Stick and a Raspberry Pi. Although the receivers and the overall setup are very simple, localization of transmitters works remarkably well.

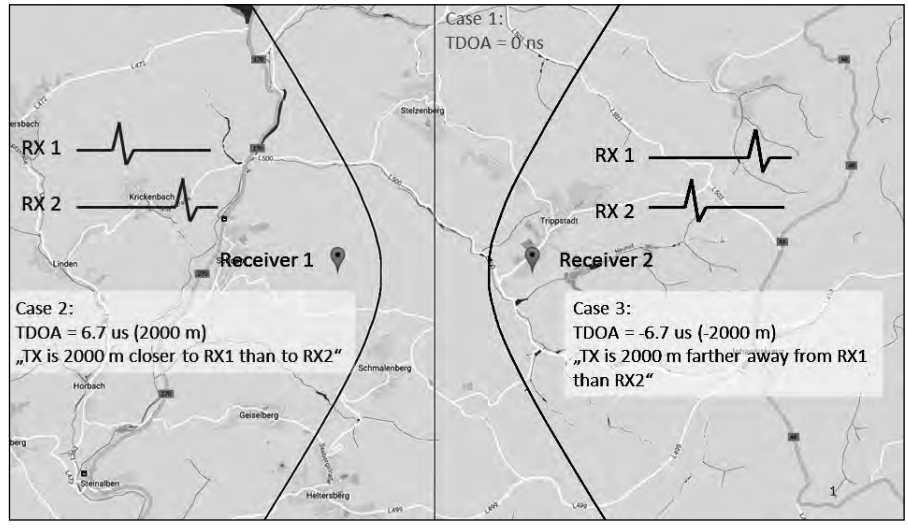

Figure 1 — Basic principle of TDOA localization using one hyperbola created by evaluating the time difference between two receivers. Here, three cases with different TDOA values are shown.

Basics of TDOA

Assume that a signal is emitted by a transmitter and is received by several receivers at different locations. Usually the signal arrives at different times at the different receivers due to the varying distances between transmitter and receivers. These differences, or TDOA values, can be measured between pairs of receivers. It should be emphasized, that we operate on the time *difference*, since any absolute arrival times in relation to transmission times are in general not available, as would be required with other localization techniques like time-of-arrival (TOA).

To understand the idea of TDOA localization, consider a simple example based on only two receivers and an unknown transmitter, see Figure 1. First, assume that the signal arrives at both receivers at the same point in time, that is, TDOA is zero seconds. Then it is obvious that the distance from the transmitter to receiver-1 is the same as to receiver-2. The transmitter must be located somewhere on a straight line in the middle between the two receivers. This is not yet a unique position, but narrows the possible positions down to a line.

Now assume a second case, where the signal arrives earlier at receiver-1 and later at receiver-2. The TDOA value now becomes non-zero. This means that the distance from transmitter to receiver-1 is smaller than to receiver-2. Note that a TDOA value can be converted to a distance by multiplication with propagation speed. In this case, the possible locations lie on a hyperbola with one of the receivers in the left focal point in Figure 1. Figure 1 (right) also shows a third case, where the signal arrives first at receiver-2, resulting in a hyperbola for the possible transmitter locations that bends to the right.

To complete localization, more than two receivers are required — at least three for two dimensional localization in a plane. The

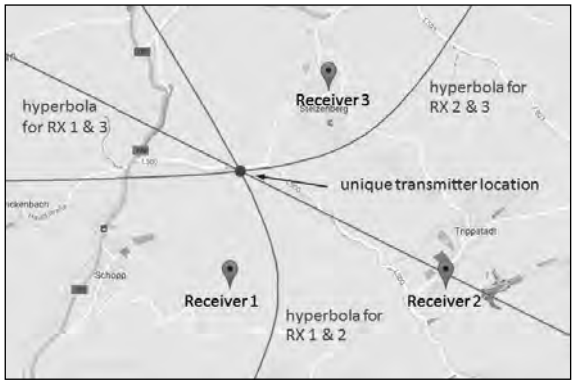

Figure 2 — Full TDOA system with three receivers yielding three hyperbolas that intersect at the transmitter location.

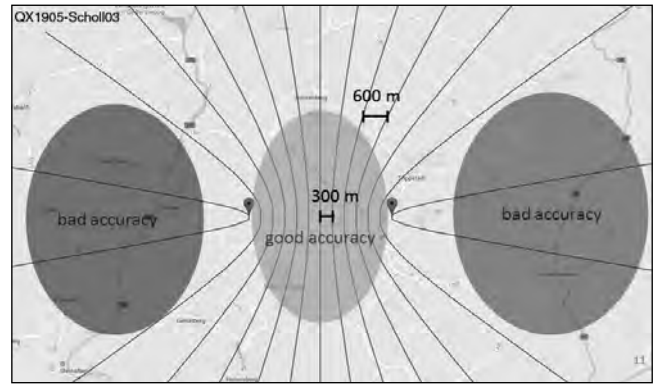

Figure 3 — The hyperbolas are for different successive TDOA values with a time resolution of 2 μs (distance resolution of 600 m) and show how time resolution translates to spatial resolution.

above described method to create hyperbolas is applied pair-wise to each receiver such that for three receivers three hyperbolas can be generated. Four receivers would yield ten hyperbolas. Ideally all hyperbolas intersect at a single location on the map, that is the transmitter position (Figure 2).

The achievable resolution and accuracy on a map does not only correspond to the resolution of the TDOA measurement. It is also largely dependent of the transmitter location relative to the receivers. Figure 3 shows that the accuracy is very good in the area roughly between the receivers, and is poor elsewhere. In general, TDOA systems perform well in the area that is surrounded by the receivers.

Although the basic idea of TDOA localization is not too complicated, some further issues need to be addressed. First, the receivers must be synchronized with each other. Second, a means of precisely determining the time differences of arrivals is needed. Third, all receivers must be placed apart, though connected and able to exchange considerable amounts of raw sampled data. These challenges must be solved to build a practical system, and will be treated in the following.

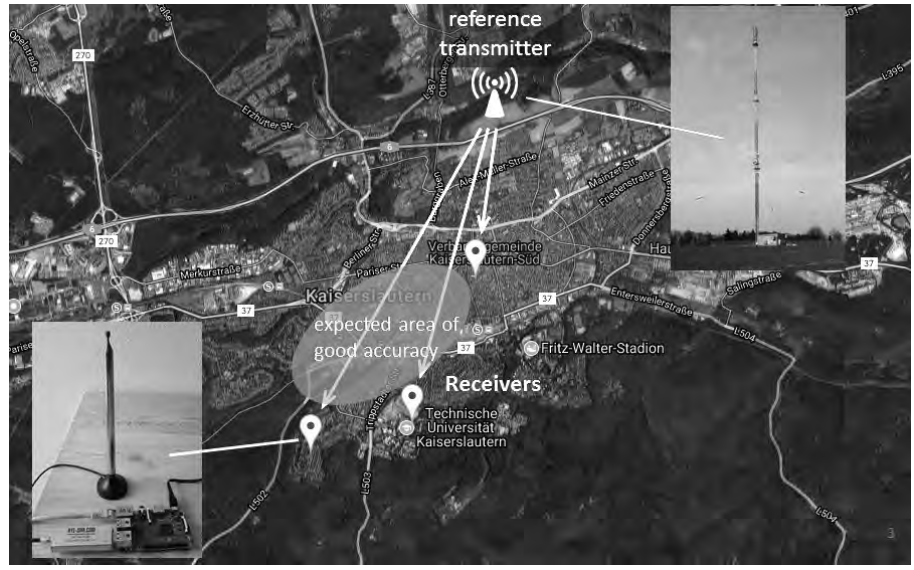

Figure 4 — TDOA system setup in the city shows the three receivers and the reference transmitter used for synchronization.

A Practical Localization System using RTL-SDRs

A complete TDOA system consists of three synchronized receivers that are connected to a central signal processing unit. In the following, a simple and cheap system for localizing signals in a city is described.

Receivers

The installed receivers are minimalistic and each consists of an RTL-SDR USB-stick (approximately US$20) and a Raspberry Pi (approximately US$40). The receivers use the simple whip antenna packaged

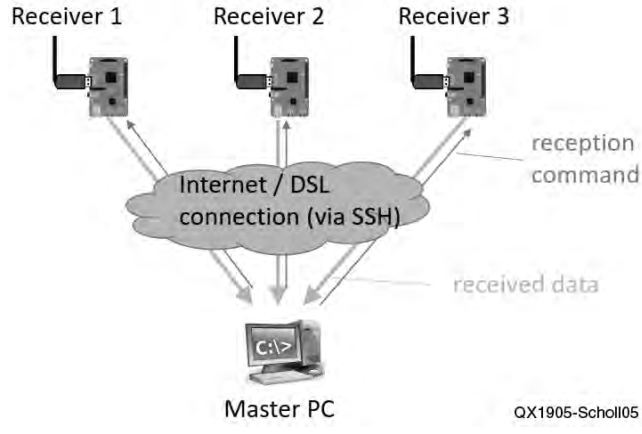

Figure 5 — The receivers are connected via internet and commanded through SSH.

with the RTL-SDR dongle. For practical reasons the antennas were placed indoors, which is suboptimal and leaves room for improvement. The RTL-SDR is capable of receiving 2 MHz of instantaneous bandwidth in a range from below 100 MHz to more than 1 GHz. This makes it a cheap and versatile general purpose SDR, capable of receiving various different types of signals.

For the experiments three receivers were deployed around in the city of Kaiserslautern, Germany. Figure 4 shows the receiver positions. For ideal placement and good accuracy the receivers should have been placed outside the city. However, no suitable internet connection could be established in the surrounding mostly forested areas. Despite the suboptimal placement, good accuracy is expected in the area roughly between the receivers.

All receivers are connected to a master PC for signal processing via the internet (Figure 5). The master PC simultaneously triggers measurements at each receiver using an SSH connection. Note, that synchronization with this methods is limited to just a few tens of milliseconds. The receivers then send the received sampled data back to master PC for further signal processing and delay analysis. The amount of sampled data can quickly become very large, since the RTL-SDR outputs 8-bit IQ-data with 2 MHz bandwidth. This creates a data rate of 2×8×2 MHz = 32 Mbps per receiver. With an available DSL upload of 1 Mbps, transferring just one second of sampled data takes approximately half a minute. Reducing the sample rate of the RTL-SDR or employing compression might relax the data rates.

It is important that the three receivers are tuned to exactly the same frequency. For that purpose the RTL-SDR frequencies are calibrated with special frequency correction bursts emitted by GSM base stations. Calibration with GSM signals is easy using the *kalibrate-rtl* software.[1]

Synchronization

A prerequisite for TDOA localization is the synchronization of the receivers. One possibility is to use a GPS receiver to discipline the Raspberry Pi internal clock. However, the system utilizes a different method using a transmitter with known location as a reference that is received well by all three receivers. There is a 2 kW DAB+ transmitter at 217 MHz in the City of Kaiserslautern that covers a large area and is perfect for synchronization.

Synchronization with a reference receiver works as follows. When the master PC triggers a measurement, each receiver first receives some samples of the reference receiver and then seamlessly switches to the unknown transmitter's signal of interest (Figure 6). For synchronization, the master PC aligns the three receptions from the three receivers on the time axis. Alignment is done in such a way that the delay in the reference signal portion corresponds to the known distances of the reference transmitter to the receivers. This creates a precise synchronization on the order of one sample period—500 ns for 2 MHz sampling. Once the received signals are synchronized (or aligned) the TDOA of the unknown signal portion is simply calculated as the remaining delay. To be precise, this technique does not synchronize the receivers themselves, but rather the received signals.

The critical point for the synchronization is the requirement to switch between the frequencies seamlessly, such that not a single sample gets lost. Otherwise, this will impair synchronization. Modifying the C library *librtlsdr*[3] (commonly used for controlling the RTL-SDR) to perform seamless frequency switching using the rtl_sdr command crashed during execution. The solution is to use a modified branch of

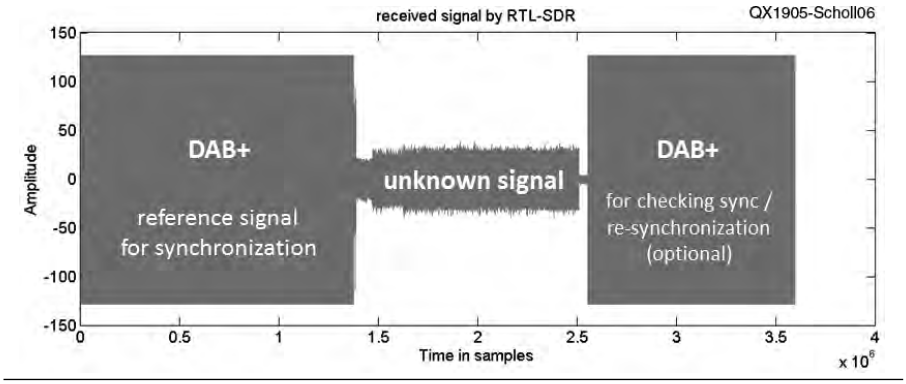

Figure 6 — A signal reception slice consists of a portion of the reference signal seamlessly followed by the unknown signal.

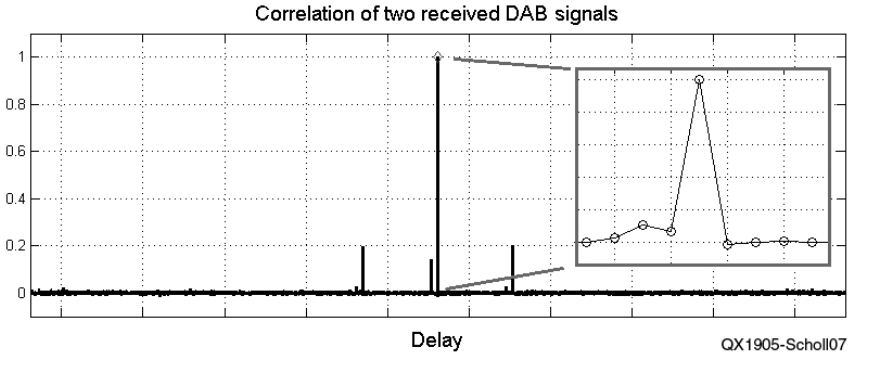

Figure 7 — Correlation of a DAB signal received by two RTL-SDRs.

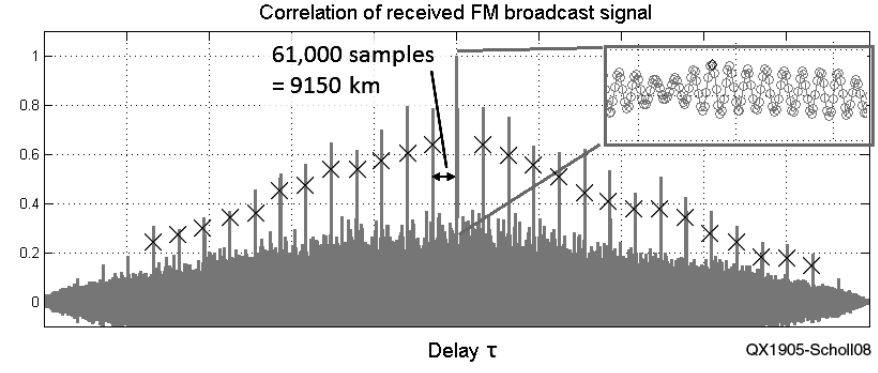

Figure 8 — Correlation of a FM signal received by two RTL-SDRs.

the *librtlsdr*, called async-rearrangements[2] as with basis. Modifying this library for seamless frequency switching worked perfectly fine and showed that the RTL-SDR can do so as well.

The modified lib *librtlsdr2freq* for switching between two frequencies is available as open source software from Github: **https://github.com/DC9ST** providing *librtlsdr-2freq* C library that allows the RTL-SDR to switch between two frequencies seamlessly; and *tdoa-evaluation-rtlsdr* Matlab script for processing data generated by *librtlsdr-2freq*.

Signal Processing

Measuring the delay between two inputs precisely is the most important operation for TDOA. For that purpose the correlation function is defined for a signal with N samples

$$Corr(\tau) = \sum_{t=0}^{N-1} s_1(t) \cdot s_2(t+\tau)$$

where s_1 and s_2 are the signals received by receiver-1 and receiver-2.

The correlation function returns for every hypothetical delay τ between the two signals a value indicating how well the two signals match. The delay value τ at which the correlation function has a peak is the delay between the signals[4].

The basic correlation function introduced above assumes real-valued data as inputs. The RTL-SDR, however, outputs complex I and Q data. Different experiments were conducted that used complex correlation, correlation on the absolute values of I and Q, and the phase difference of complex I and Q data. It turned out that the method using phase differences was most suitable for a wide range of different signals[5].

In practice further challenges remain. The quality of correlation — a single unique peak is desired — depends on many factors such as signal bandwidth, periodicity, multi-path propagation, noise, transmitted content and the fact that signals were processed through different receivers. Figures 7 and 8 show the correlation functions of real-world signals captured with two RTL-SDRs placed at different locations. The DAB signal has a very good correlation with a dominant and distinct peak. The correlation function for the FM signal is of poorer quality, showing many outstanding spikes and no distinct peak sample.

The problem identifying a single sample as correlation peak can be improved by simply smoothing the correlation function with a moving average filter.

The problem of multiple peaks can often be solved by considering the values on the time-delay axis of the correlation function. For the FM signal in Figure 8 the distance between the peaks is comparably large, around 61,000 samples, which corresponds to a difference in distance of 9,150 km. However, the maximum possible delay is the distance between the two receivers, here, a few kilometers. Therefore any peaks that correspond to positive or negative delays greater than the receiver's distance can be discarded. Often this leaves just a single peak even with correlation functions that look very difficult at first sight.

The RTL-SDR sample rate of 2-mega-samples per second (Msps) over a 500 ns period restricts the time delay measurement to a resolution of 150 m, which corresponds to a localization resolution of a minimum of 75 m. Recall that resolution is also dependent on the transmitter position relative to the receivers. One possibility to further increase the theoretical resolution of delay measurement is by using interpolation that inserts additional samples between two samples of the original signal. However experiments showed that in practical operation the gain in accuracy was very little, suggesting that the system accuracy is limited by other factors.

With the correlation function available

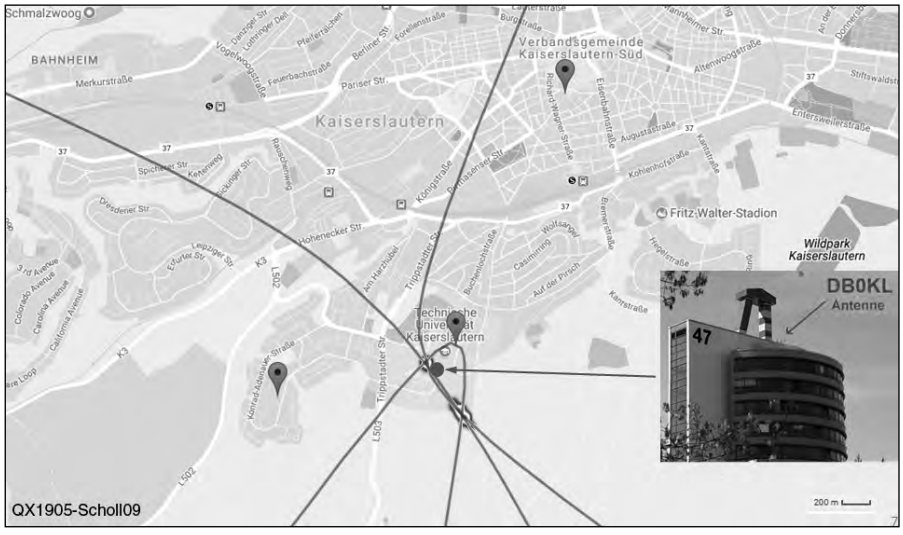

Figure 9 — Localization of a DMR repeater signal at 439 MHz. Two positions are possible, but are very close to the true location.

Figure 10 — Localization of a mobile signal at 922 MHz. All base stations are marked by a star. The signal probably originates from the encircled star.

Figure 11 — Localization of an unknown signal at 391 MHz (approximately 12 kHz bandwidth). The measured position is located near the local post office and the train station.

Figure 12 — Localization of a FM broadcast signal at 96.9 MHz, where the transmitter is located to the side.

for measuring the delay or TDOA, and with synchronized receptions, the overall signal processing for TDOA localization can be summarized as follows.

- Receive signals, transfer them to the master PC and consider them pair-wise for further processing;
- Synchronize the received signals;
- Optionally up-sampling by interpolation;
- Calculate correlation of reference signal portion;
- Discard invalid peaks of correlation function;
- Use measured delay to synchronize signals in time;
- Measure unknown signal;
- Determine TDOA in sample and distance;
- Calculate hyperbola using geometry;
- Create a map with html and JavaScript to display all three hyperbolas.

The signal processing was implemented as a *Matlab script*[6].

Results

The results show the localization of four different transmitters of various signals. A DMR signal at 439 MHz (Figure 9) from Amateur Radio repeater DBØKL, a mobile phone signal (Figure 10) at 922 MHz, and an unknown signal (Figure 11) at 391 MHz, have been localized with remarkably high precision. An additional FM signal at 96.9 MHz originates from a transmitter located outside the receiver array (Figure 12), which makes exact localization naturally difficult. In this case, however, TDOA still can identify the incoming direction and therefore serves as simple direction finder. Overall, the results are remarkably good and show that localization is possible with this simple setup.

Further Development

Since the presented system is simple, improvements can be made to increase accuracy, reliability and speed: A better radio with higher sampling rate and more stable clocks, better antenna and better placement of the antenna may improve accuracy. The problem of the large amount of data could be tackled by using a lower sample rate or using data compression.

Stefan Scholl, DC9ST, was originally licensed in 2006, as a German Class A license. He received the Diploma in electrical engineering in 2010 from University of Kaiserslautern, Germany, where he worked for 6 years as a researcher in the area of forward error correction for communication systems. He completed his PhD in 2018. Currently he is a development engineer for radar technology at Hensoldt (formerly Airbus Defence and Space). Stefan's interests include homebrew equipment and hardware and algorithms for software defined radio.

Notes

[1]**https://github.com/steve-m/kalibrate-rtl**.
[2]**https://github.com/mutability/librtlsdr/tree/async-rearrangements**.
[3]**https://github.com/steve-m/librtlsdr**.
[4]S. W. Smith, *The Scientist and Engineer's Guide to Digital Signal Processing.*, 1997.
[5]Further information: **www.panoradio-sdr.de**.
[6]**https://github.com/DC9ST**.

Jim Koehler, VE5FP

2258 June Rd., Courtenay, BC V9J 1X9, Canada; **jark@shaw.ca**

Measure Crystal Parameters Using a Vector Impedance Meter

Crystal parameters can be automatically determined from measurements of impedance.

Vector impedance meters, often called Network Analyzers, are valuable tools for those interested in designing and constructing antennas, in RF design and implementation, and in measuring RF component parameters. Professional vector impedance meters have been very costly but the amateur fraternity has come up with a number of excellent, and affordable designs[1-4].

I was inspired to design my own vector impedance meter by Yury Kuchura's, EU1KY, use of the Si5351A single chip dual-output signal source and by Michael Knitter's, DG5MK, use of the MCP3911 dual-channel A/D converter. The Si5351A can provide stable, accurate frequencies over a wide range up to 200 MHz, and the MCP3911 is a very low-cost 16-bit A/D converter that digitizes two channels sampled simultaneously. My own design was meant to mainly function as a simple component tester for measuring inductance and capacitance over a wide range of frequencies. Of course, it can also measure antenna or other network impedances. It uses 1% resistors in the bridge measuring network and, due to careful layout, has a measurement accuracy of just a few percent without further calibration. My design worked very nicely and I was greatly encouraged by its accuracy, repeatability and frequency stability. It was a natural next step to think of using the instrument to make crystal parameter measurements. Many of the previously cited vector impedance meter designs might also be suitable for this purpose so I am going to describe how crystal parameters might be automatically determined from measurements of impedance.

The electrical behavior of a quartz crystal can be described by the equivalent circuit shown in Figure 1. There are more complicated circuits possible but most crystals in the HF range are well described by this simple circuit. All four circuit elements must be measured if a design, such as a crystal filter, is to be synthesized. The amateur literature has a large body of articles about, and designs for measuring these four values[5-8] but none, I think, of how to use a vector impedance meter to do so.

Desirable Features of a Vector Impedance Meter

For my design, I wanted to build just a basic 'vector impedance engine' controlled by an external computer via a simple serial interface running at 115,200 baud. The basic engine would take commands to set the frequency, set scan bounds, make the measurements, and the external computer would do the heavy lifting of producing nice graphs and complex analysis.

The basic engine covers the frequency range from 1 MHz to 200 MHz, can sample at the rate of about 18 measurements per second and has a frequency drift, after 20 minutes of warm-up, of less than 10 Hz per hour at 10 MHz. This engine is controlled by an ARM-7 32-bit microprocessor. The computation time needed to calculate an impedance or admittance is negligible compared to the time taken doing the A/D sampling needed to determine the value. The firmware for the engine controller is written in C.

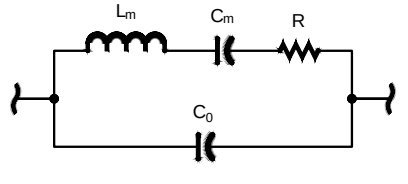

Figure 1 — The equivalent circuit of a crystal.

From the viewpoint of measuring crystals, it is desirable to sample impedance versus frequency as quickly as possible. Frequency stability is a prime consideration for accuracy but speed of sampling is important from the viewpoint of minimizing the time needed to completely measure one crystal's parameters. The accuracy of the measured impedance should be better than a few percent. The series resistance of a 'good crystal' in the HF range will typically be less than 10 Ω so the impedance meter must be accurate in this range. It is not necessary that the impedance meter be accurate for impedances greater than a few hundred ohms.

Crystals and Their Parameters

Figure 2 shows the admittance plot over a

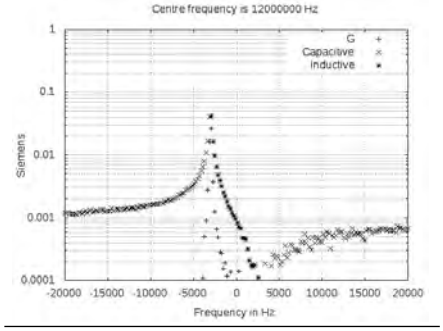

Figure 2 — Plot of admittance (+) *vs.* frequency for a crystal in its fixture. There are capacitive (x) and Inductive (*) ranges.

40 kHz frequency span of a nominal 12 MHz HC49/U crystal in the jig as generated by my impedance meter. When a crystal is in the jig, its series circuit will be paralleled by C_0 , the stray capacitance of the jig and any residual stray admittance in the impedance meter itself. The admittance plot here is convenient because these stray admittances will just add to that of the crystal. We can compensate for them by just measuring them separately and then subtracting them from the measured values to get the admittances of the crystal alone. For my impedance meter, this total admittance was purely capacitive; it is the net instrument susceptance.

The measurement of the instrument susceptance can best be done at a high frequency. In my case this is at 200 MHz. The capacitive susceptance was measured to be 12.8 mS which corresponds to a capacitance of 10.2 pF. At 12 MHz this looks like 769 μS and so this value should be subtracted from the measured values across the spectrum of the scan.

Figure 3 shows a plot of the phase of the admittance over the frequency span for the same crystal. At frequencies below the series resonance, the phase is more or less constant at close to +1.57 radians (+90°) as one would expect from a simple capacitor. Near the series resonance, it rapidly goes down to about -1.57 radians (-90°), wobbles about down there but stays inductive and then goes back up to +1.57 radians, near parallel resonance and stays there at higher frequencies. After compensating for the susceptance of the instrument, this plot will look very much different and the frequency at which the phase goes through zero will be changed very slightly[9].

Measuring Crystal Capacitance

Normally, when measuring the parameters of a batch of crystals one selects a few, measures them with a capacitance meter and assumes that the average value is applicable to every crystal in the batch. There is nothing wrong with this but it is possible to measure C_0 with just the impedance meter. First, take the crystal from the jig and the measure the capacitive susceptance at some high frequency. In my case, this will be near 200 MHz; call this B_1. Then, place the crystal back in the jig and measure the susceptance again at the same frequency. Call this value B_0. Then the crystal capacitance C_0 will be,

$$C_0 = \frac{B_0 - B_1}{2\pi f} \qquad (1)$$

Determining Series Resonant Frequency, *R* and *Q*

Once we've determined the instrument susceptance and subtracted it from the admittance values, if we can re-plot the measurements. The phase plot Figure 4 shows the phase is near 90º for frequencies below series resonance, passes quickly through zero at resonance and then is near -90° for higher frequencies. There is now no parallel resonance so in Figure 5 there is a single admittance peak. Figures 6 and 7 show the phase and admittance over a narrower frequency span of ±200 Hz. These narrower-span plots show the behavior over the important central region of the crystal response.

The series resonant frequency in Figure 6 is that at which the phase is zero — here close to the graph's zero frequency of 11.997000 MHz. The value of Q can be determined by measuring the bandwidth between the two frequencies at which the phase is ±45°. Q is then the value of the resonant frequency divided by this bandwidth. Measuring crudely from this graph, that bandwidth is approximately 90 Hz so the Q is approximately 130,000.

More accurate estimates of these numbers could be made by scanning over a much smaller frequency range. It is inconvenient to measure a batch of crystals and determine their parameters by plotting a pair of graphs for each crystal and then determining the parameters by making measurements from those graphs. There has to be a better way.

In the vicinity of resonance, where the excursions in frequency are small compared to the center frequency, the phase ϕ in radians is given to a very good approximation by,

$$\phi = \arctan\left(\frac{2Q}{f_0}(f_0 - f)\right) \qquad (2)$$

where f_0 is the series resonant frequency and f is the frequency of measurement. Q is,

$$Q = \frac{2\pi f_0 L_m}{R}$$

Similarly, over the same small frequency region, the value of the conductance G (to a very good approximation) is,

$$G = \frac{G_0}{1 + \left(\frac{2Q}{f_0}(f_0 - f)\right)^2} \qquad (3)$$

where G_0 is the conductance at the series resonant frequency. It is equal to $1/R$ in Figure 1.

The plotting package *gnuplot* allows one to fit a function to data. Such a fit for the phase data is shown in Figure 6. Eqn (2) may be rewritten as:

$$\phi = \arctan\left(a(b - f)\right) \qquad (4)$$

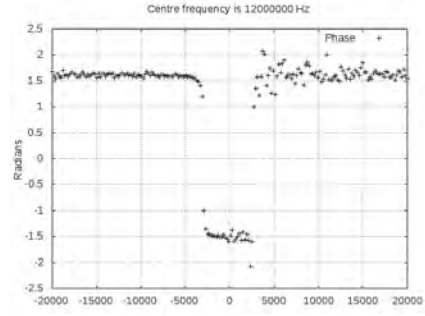

Figure 3 — Plot of the phase of the admittance for the same crystal in its fixture.

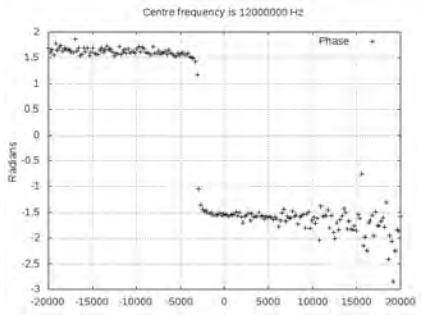

Figure 4 — Plot of the phase of the admittance after correction for fixture and internal capacitance.

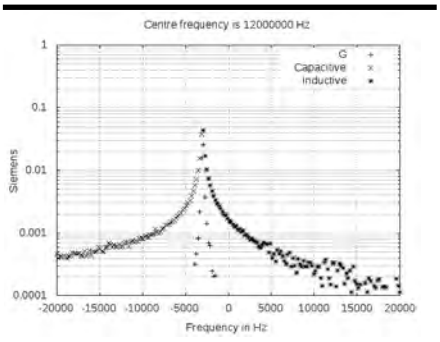

Figure 5 — Plot of admittance *vs*. frequency for crystal, after corrections.

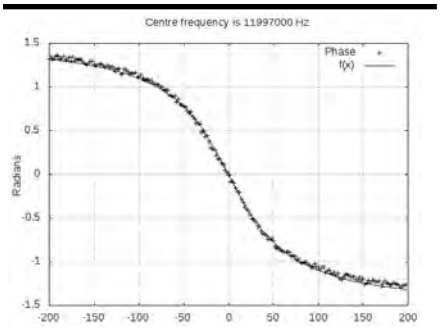

Figure 6 — Plot of the phase of the admittance over the small region near resonance, after corrections.

and the data points in the graph can be fitted to give a and b,

$$a = \frac{2Q}{f_0} \quad \text{and} \quad b = f_0$$

The parameters of the fit give the value of a as 0.0198 and the value of f_0 as -0.2 Hz.

Similarly, Eqn (3) may be rewritten as,

$$G = \frac{c}{1+\left(a\left(b-f\right)\right)^2} \qquad (5)$$

and solved for a, b and c. Here $c = G_0$. The best fit values are plotted in Figures 6 and 7 as solid lines. The *gnuplot* fitting algorithm uses the Levenburg-Marquardt technique[10] and in these particular cases the solutions converged quickly because the fits were so good. Since the graphs were drawn with 11.997000 MHz as zero, the actual crystal series resonant frequency is 0.2 Hz lower than this, and Q turns out to be about 118,800. G_0 = 0.103 gives a value of R = 9.7 Ω. These graphs were made, and the curve-fit, for a scan of 200 frequencies in the ±200 Hz interval.

One might now ask how many data points are needed to get a good estimate for the parameters? The estimate of the uncertainty from the *gnuplot* program for Figure 6 was about ±0.4 Hz in the resonant frequency and about ±1,100 in Q. Rescanning over the same frequency interval with just 21 data points gives the graphs shown in Figures 8 and 9. Here the fit yields a resonant frequency of -0.3 Hz and the value of Q works out to be 115,200 with an estimated uncertainty of about ±0.7 Hz in frequency and about ±3,000 in Q. A scan over 21 data points takes just over a second with my impedance meter whereas a scan of 200 data points would take about 11 seconds. One can conclude that taking samples at more than 10 to 20 frequencies does not significantly improve the accuracy of the parameter determination and hence the shorter scan lengths are good enough.

Using *gnuplot* to fit the equations to the data points, although useful for understanding what is going on, is a cumbersome procedure. Fortunately, there are a number Python library packages for curve-fitting that use the Levenburg-Marquardt method[11]. So, to automatically measure crystal parameters with an impedance meter, we merely need to scan the impedance in the frequency region near the series resonant frequency, convert impedance to admittance, remove the instrument systematic errors and then use the data by finding the best fit to Eqns (4) and (5) to determine R, Q and f_0.

For my impedance meter, I already had built in a command that will do the scan, correct for the instrument susceptance, and then output a table of frequency and admittance over the frequencies sampled. The time depends on the number of frequencies in the scan. I usually opt to use 11 or 21, and the times are about just over a half-second and just over one second respectively. The external computer routine that starts the process takes a fraction of a second to download the data from the impedance engine, do the curve fitting, solve for R, Q and f_0 and write the these output values to a text file. The curve fitting takes appreciably longer when using the R-Pi version of the impedance meter.

Programs and Techniques

I have written several Python programs to measure crystal parameters automatically. For a new batch of crystals, especially if you have bought them from a surplus supplier, the nominal frequency stamped on the case may not be very accurate. For example, the batch of crystals I bought that were nominally 12 MHz turned out to have a series-resonant frequency very close to 11.997 MHz, 3 kHz lower than the nominal frequency. So it is prudent to first do a general scan of impedances or admittances over a fairly wide frequency range for a few crystals to determine the approximate series frequency. I wrote a Python program that does just that. It starts with a specified nominal frequency and a width that is too wide to be useful for accurate parameter measurement. It returns the actual measured series resonant frequency and gives a frequency range that will result in a phase range of just more than ±1 radian. Those numbers can then be used in the programs that make the measurements.

For testing I have written a program that does a scan over a more limited range and then plots graphs similar to Figure 8 and 9.

Finally, I have written a program that is suitable for measuring a batch of crystals. It prompts for an identification number for each crystal, and writes that number along with the values for f_0, Q and R as a line in a text file. This text file has comma-separated values (CSV) and so can be read into a spread sheet where it can be easily sorted for frequency, Q or even R. The frequency is expressed in integral Hz, Q is rounded off to hundreds and R is rounded off to one decimal place. I have made the program available on the **www.arrl.org/QEXfiles** web page so that those who wish to amend it to use with their impedance meters can see how I did it[12].

The Basic Engine

Figure 10 shows the basic engine powered by a 12 V wall wart. The internal circuitry is built using surface-mount components on a single pc-board mounted on the under side of the box lid. The box itself has just a voltage regulator, an input power jack and a stereo audio jack for the 3.3 V logic level serial data interface. This is connected to the controlling computer via a logic level to USB adapter going to a USB port on the computer. All of the software for the controlling computer was written in Python and I have used these programs either in a laptop or desktop computer.

I made a second version of the instrument in which the controlling computer was a

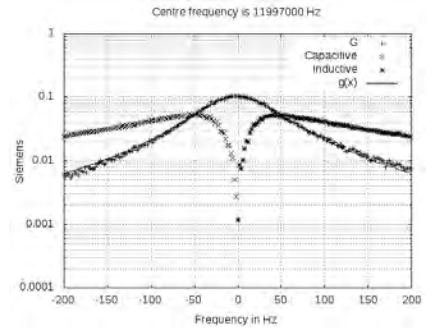

Figure 7 — Plot of the admittance over a small region near resonance, after corrections.

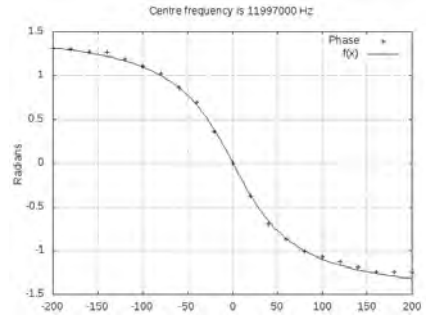

Figure 8 — Plot of phase showing best fit to the measured phases.

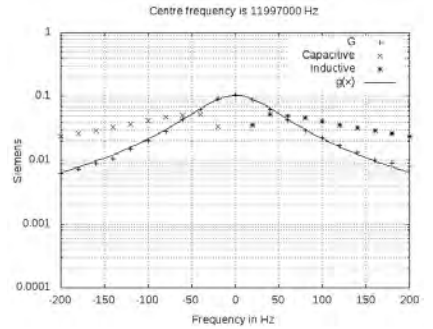

Figure 9 — Plot of admittance showing best fit to the measured conductance.

Raspberry Pi Zero W enclosed with the engine in a plastic box to allow the R-Pi to connect to my Local Area Network via Wi-Fi. The R-Pi is considerably slower than a modern laptop in running the Python programs but it does the job and the setup is considerably more compact.

My impedance meter has a BNC test socket. I was able to buy some BNC adapters from China that are very suitable for making a jig to hold crystals during measurement. Figure 11 shows the BNC adapter on the left and my addition to it: two machined pins broken from an IC socket soldered to one of the side pins and the center pin, on the right. I adjusted the spacing of the machined pins on the BNC adapter to match the wire separation of HC18/U or HC49/U crystals.

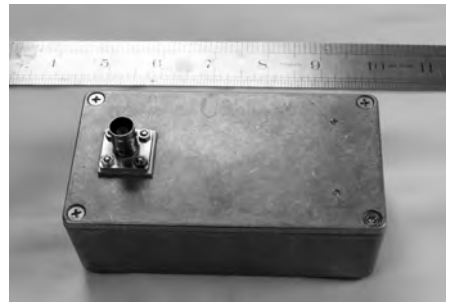

Figure 10 — Photo of the impedance meter engine with serial interface.

Figure 11 — Photo showing small BNC adapter on the left and, on the right, the added contacts for measuring crystal parameters.

Comments

Many home-brewers want to use crystal filters and therefore need to be able to measure crystal parameters. To be sure, one can build a piece of test apparatus to make these measurements, but anyone who already has a vector impedance meter can use the method proposed here instead. I hope that interested readers will find the example of the program cited above useful in that regard.

In the Amateur Radio literature, batches of crystals have mostly been measured one crystal at a time and one measurement at a time. Just a few measurements are made and then the parameters are derived from them. For example, a recent method uses three frequency measurements of a oscillator with and without an extra series capacitor[13]. The parameters Q, R and f_0 are determined from these three measured frequencies. In the method I have described here, admittances are measured at a number of frequencies, typically 21, and so the parameters are determined on the basis of a larger number of measurements. Since, in general, accuracy is improved by the square root of the number of measurements, one could expect that random errors would tend to average out. Remember that this averaging does not reduce systematic errors. Nevertheless, it should greatly improve the consistency of the results.

In order see how consistent the results are, I measured the same crystal, 24 times in the batch fitting program. This was one of the 12 MHz nominal crystals. In the batch (the same crystal measured 24 times), the average f_0 had a standard deviation of 0.56 Hz, the average Q was 102,188 with a standard deviation of 986. The average R was 11.06 Ω with a standard deviation of 0.14 Ω. These numbers suggest that Q and R are determined with an accuracy of about 1%.

Finally, sharp-eyed readers may have noticed that Eqn (5) gives all three parameters and so may ask why it is necessary to use Eqn (4) to determine resonant frequency and Q. Indeed, since an impedance meter, uncorrected for stray capacitance, can give the conductance *vs.* frequency directly, and since Eqn (5) uses only the conductance, why is it necessary to bother with the stray capacity correction in the first place? The answer to both these questions is that, in principle, it really is unnecessary to: (a) compensate for the stray capacitance of the jig and crystal and, (b) bother with looking at the phase data.

However, Eqn (4) gives a very accurate assessment of the resonant frequency and Q because the phase varies so rapidly with frequency in the vicinity of the series resonant frequency. It is more accurate than those parameters derived from Eqn (5) where the conductance varies more slowly with frequency. Since the calculation of best-fit takes negligible time, it seems to me that the potentially greater accuracy is worth the trouble of writing a few extra lines of code in the program.

I would like to thank my friend, Tom Alldread, VA7TA, for his useful comments. I would like to also thank Horst Steder, DJ6EV, and Jack Hardcastle, G3JIR, for their wonderful program[14] for designing filters once the characteristics of one's batch of crystals is known.

Jim Koehler, VE5FP, earned his first ham license at age 15 in 1952. He completed undergraduate university, then was awarded a post-graduate degree in Australia. He returned to Canada in 1966, and became Professor of Physics and Engineering Physics at the University of Saskatchewan, and did research in upper-atmospheric physics. After retiring in 1996, he and his wife moved to Vancouver Island to enjoy Canada's best climate. Jim shares a hobby interest in electronic design with friend Tom Alldread, VA7TA. Both have extensive "junk boxes" and so are able to scrounge parts from one another freely, and cooperate with each other in taking advantage of all the new integrated circuits, which make life so much easier than when they were much younger.

Notes

[1]The N2PK VNA, see **n2pk.com**.

[2]T. C. Baier, DG8SAQ, "A Low Budget Vector Network Analyzer for AF to HF", *QEX*, Mar./Apr., 2007, pp. 46-54.

[3]M. Knitter, DG5MK,"The DG5MK IV Meter – An Accurate Antenna Analyzer", *QEX*, May/Jun., 2017, pp. 3-15.

[4]The AA-V3 antenna analyzer, **bitbucket.org/kuchura/eu1ky_aa_v3/wiki/home**.

[5]J. Kortge, K8IQY, "Simplified Tools and Methods for Measuring Crystals", AmQRP Homebrewer, Issue #7, 2006.

[6]J. Hardcastle, G3JIR, "Quartz Crystal Parameter Measurement", *QEX*, Jan./Feb., 2002, pp. 7-11.

[7]R. Evans, KJ6PO, "Crystal Parameter Measurement and Ladder Crystal-Filter Design", *QEX*, Sep./Oct., 2003, pp. 38-43.

[8]J. Koehler, VE5FP, "The Shunt Method for Crystal Parameter Measurement", *QEX*, Jul./Aug. 2010, pp. 16-25.

[9]A. Bloom, N1AL, Letters to the Editor, *QEX* Sep./Oct. 2008, pp. 41-42, and Jan./Feb. 2010, pp. 37-38.

[10]**https://en.wikipedia.org/wiki/Levenberg%E2%80%93Marquardt_algorithm**.

[11]**https://docs.scipy.org/doc/scipy/reference/generated/scipy.optimize.curve_fit.html**.

[12]See "fit.py" programs, **www.arrl.org/QEXfiles**.

[13]R. J. Harris, G3OTK,"An Automated Method for Measuring Quartz Crystals", *QEX*, Nov./Dec., 2013, pp. 3-8.

[14]H. Steder, DJ6EV and J. Hardcastle, G3JIR,"Crystal Ladder Filters for All", *QEX*, Nov./Dec., 2009, pp. 14-18.

Technical Note

Measuring Characteristic Impedance of Coax Cable in the Shack - Another Approach

John Flood, K4DLX, in his "Measuring Characteristic Impedance of Coax Cable in the Shack" *QEX* Technical Note[1] provided a very handy means for measuring the characteristic impedance of a transmission line. Although John's method is intended for cases where Z_0 is real or nearly so, his method can be extended[2] to lines that exhibit complex Z_0. John pointed out that the input impedance of a shorted one-eighth wavelength line will be jZ_0. If we assume that

$$Z_0 = R_0 + jX_0$$

we have:

$$\begin{aligned} Z_{in} &= jX_0 \\ &= j(R_0 + jX_0) \\ &= -X_0 + jR_0 \quad . \end{aligned}$$

We can verify these results using *TLW*[3] or *GNU Octave code*[4] from "Octave for Transmission Lines". Both of these utilities accept the velocity factor and the length of the transmission line in meters or feet as inputs rather than wavelength. We need the wavelength of the line at the frequency of interest. We can calculate that as follows:

$$\gamma = \frac{cVF}{f}$$

where

γ is the wavelength, m

c is the speed of light in free space, 299,792,458 m/s

VF is the velocity factor of the line

f is the frequency, Hz.

If, for example, $VF = 0.66$, and $f = 7$ MHz, then

$$\gamma = \frac{299,792,458 \times 0.66}{7 \times 10^6}$$
$$= 28.266 \quad \text{m.}$$

so

$$\frac{\gamma}{8} = 3.533 \text{ m},$$

rounded off to four significant figures.

We'll assume that $Z_0 = 73 - j12\ \Omega$. Entering that and the information above into *TLW*, we get $Z_{in} = 12.01 + j73.09\ \Omega$. We can obtain Z_0 from that by reversing the real and imaginary parts and changing the sign of the real part as we make the change. The results we calculated are accurate to within the expected round-off error. No practical transmission line would exhibit such a large X_0 at 7 MHz, but this example is intended only to prove the method.

What if the attenuation is not zero? We'll postulate a loss of 4 dB per 100 m, typical of some RG-58 cables. When we add that to the transmission line details in *TLW*, the input impedance changes to $Z_{in} = 14.38 + j72.66\ \Omega$, close enough if we are trying to determine or verify the Z_0 of a line.

Note that most of the variation is in the real part of the input impedance. The variation in the imaginary part — which maps to the real part of Z_0 — is relatively small, indicating that application of this technique to real lines should be sufficiently accurate for most practical purposes even when loss in the cable is not ignored.

Either *TLW* or the *GNU Octave* code can also be used to verify or experiment with this method for transmission lines whose Z_0 is real. — *73, Maynard Wright, W6PAP,* **m-wright@eskimo.com**.

Notes

[1] J. Flood, K4DLX, Technical Notes: "Measuring Characteristic Impedance of Coax Cable in the Shack," *QEX*, Nov./Dec., 2017, pp. 35-36.

[2] M. Wright, W6PAP, "Octave for Complex Z_0," *QEX*, May/June, 2017, pp. 21-25.

[3] *TLW, Version 3.1*, "*The 2018 ARRL Handbook for Radio Communications*," available from your ARRL dealer or the ARRL Bookstore, ARRL item no. 0444. Telephone 860-594-0355, or toll-free in the US 888-277-5289; **www.arrl.org/shop**; **pubsales@arrl.org**.

[4] M. Wright, W6PAP, "Octave for Transmission Lines," *QEX*, Jan./Feb. 2007, pp. 3-8.

Send your short *QEX* Technical Note to the Editor, via e-mail to qex@arrl.org. We reserve the right to edit your Note for clarity, and to fit in the available page space. "*QEX* Technical Notes" may also appear in other ARRL media. The publishers of *QEX* assume no responsibilities for statements made by correspondents.

Errata

In Tom Alldread, VA7TA, "Wide Dynamic Range Field Strength Meter" *QEX* Jan./Feb. 2019 there are errors in Figure 5. Specifically C11 is shown grounded and should instead be shown in parallel with R12. Additionally some of the pin numbers for U2 are incorrect. The corrected Figure 5 schematic and additional files are posted online in QEXfiles for January/February 2019. We regret the error.

In David M. Collins, AD7JT, "The Ultimate Keyer" *QEX* Jan./Feb. 2019, readers may obtain copies of the source code for the Ultimate Keyer firmware from the author by email **ad7jt@cox.net**. This information was inadvertently omitted from the article. We apologize for any inconvenience this may have caused.

In Phil Salas, AD5X, "Low-Cost Low-Distortion 2-Tone Test Oscillator for Transmitter Testing", *QEX* Jan./Feb. 2019, the audio output is mistakenly shown connected to the collector of the output transistor. Instead the output should be taken via the 0.1 µF capacitor from the junction of the emitter and the 3.3 kΩ resistor. Thanks to Dave Hershberger, W9GR, for spotting the error.

Upcoming Conferences

2019 Central States VHFS Society, Inc. Conference

July 25 – 27, 2019
Lincoln, Nebraska
www.2019.CSVHFS.org

Call for Papers & Presentations

The Central States VHF Society is soliciting papers, presentations, and poster displays for the 53rd Annual CSVHF Society Conference to be held in Lincoln, Nebraska, July 25 – 27, 2019, at the Country Inn and Suites Lincoln North Hotel and Convention Center. Papers, presentations, and posters on all aspects of weak-signal VHF and above Amateur Radio are requested. You do not need to attend the conference, nor present your paper, to have it published in the Proceedings. Posters will be displayed during the two days of the Conference.

Topics of interest include (but are not limited to): antennas, including modeling/design, arrays, and control; pre-amplifiers (low noise); test equipment, including homebrew, commercial, and measurement tips and techniques; construction of equipment such as transmitters, receivers, and transverters; RF amplifiers including single-band and multi-band vacuum tube, solid state, and TWTAs; propagation, including ducting, Sporadic E, and tropo, ionospheric, meteor, or rain scatter; regulatory topics; operating, including contesting, roving, and DXpeditions; EME (moonbounce); Digital Signal Processing; software defined radio; and digital modes such as WSJT-X, FT8, JT65, etc.

Generally, topics not related to weak-signal VHF such as FM repeaters and packet-radio are not accepted for presentation or publication. However, there are always exceptions. If you have any questions about the suitability of a particular topic, please contact the proceedings or presentation coordinators listed below.

Deadline for submissions

Proceedings: Submit your paper(s) to Kent Britain at **wa5vjb@flash.net** no later than Sunday, May 12, 2019.

Presentations: Coordinate your presentation with Donn Baker at **wa2voi@arrl.net** no later than Sunday, June 2, 2019. With coordination, presentations and posters may be delivered at the conference.

Further information is available on the CSVHF society website, including "Guidance for Proceedings Authors," "Guidance for Presenters," and "Guidance for Table-Top/Poster Displays."

GNU Radio Conference 2019

September 16 – 20, 2019
Huntsville, Alabama
https://www.gnuradio.org/grcon/grcon19/

The GNU Radio Conference 2019 will be held at the "Huntsville Marriott at the Space & Rocket Center." This conference celebrates and showcases the substantial and remarkable progress of the world's best open source digital signal processing framework for software-defined radios. In addition to presenting GNU Radio's vibrant theoretical and practical presence in academia, industry, the military, and among amateurs and hobbyists, GNU Radio Conference 2019 will have a very special focus.

Summer 2019 marks the 50th anniversary of NASA's Apollo 11 mission, which landed the first humans on the Moon. GNU Radio Conference selected Huntsville, AL, USA as the site for GNU Radio Conference 2019 in order to highlight and celebrate space exploration, astronomical research, and communication.

Space communications are challenging and mission critical. Research and development from space exploration has had and continues to have far-reaching effect on our communications gear and protocols.

Registration and an online and mobile-friendly schedule will be posted at the conference website.

Call for All!

We invite developers and users from the GNU Radio community to present your projects, presentations, papers, posters, and problems at GNU Radio Conference 2019. Submit your talks, demos, and code! Please share this "Call for All" with anyone you think needs to read it.

To submit your content for the conference, visit our dedicated conference submission site at: **https://openconf.org/GRCon19/openconf.php**

First round closes 1 July 2019. If accepted, your content will be immediately scheduled. Final round closes 1 September 2019. Space permitting. Pun intended.

If you have questions or need assistance with OpenConf, or have content that doesn't quite fit and you want to talk it over, please write **grcon@gnuradio.org.**

Special focus awards given to all accepted work with Space as a topic. Topics may include but are not limited to: space (including ground stations); Amateur Radio; radio astronomy; atmospheric research; theoretical work; practical applications; aviation; biomedical; citizen science; Digital Signal Processing; education; radio interface; machine learning; cognitive radio; transportation, and wireless security.

ARRL and TAPR 38th Digital Communications Conference (2019)

September 20 – 22, 2019
Detroit, Michigan
www.tapr.org/dcc.html

Mark your calendar and start making plans to attend the premier technical conference of the year, the 38th Annual ARRL and TAPR Digital Communications Conference to be held September 20 – 22, 2019, in Detroit, MI. The conference location is the Detroit Metro Airport Marriott Hotel.

The ARRL and TAPR Digital Communications Conference is an international forum for radio amateurs to meet, publish their work, and present new ideas and techniques. Presenters and attendees will have the opportunity to exchange ideas and learn about recent hardware and software advances, theories, experimental results, and practical applications.

Topics include, but are not limited to: Software Defined Radio (SDR), digital voice, digital satellite communications, Global Position System (GPS), precision timing, Automatic Packet Reporting System™ (APRS), short messaging (a mode of APRS), Digital Signal Processing (DSP), HF digital modes, Internet interoperability with Amateur Radio networks, spread spectrum, IEEE 802.11 and other Part 15 license-exempt systems adaptable for Amateur Radio, using TCP/IP networking over Amateur Radio, mesh and peer to peer wireless networking, emergency and Homeland Defense backup digital communications, using Linux in Amateur Radio, updates on AX.25 and other wireless networking protocols.

Call for Papers: Technical papers are solicited for presentation at the ARRL and TAPR Digital Communications Conference and publication in the Conference Proceedings. Annual conference proceedings are published by the ARRL. Presentation at the conference is not required for publication. Submission of papers are due by July 31, 2019 and should be submitted to

Maty Weinberg, ARRL
225 Main Street
Newington, CT 06111
or via the Internet to **maty@arrl.org**

Microwave Update 2019

October 3 – 5, 2019
Dallas, Texas
www.microwaveupdate.org

The North Texas Microwave Society would like to invite you to the annual Microwave Update Conference to be held October 3 – 5, 2019 at the Hilton Garden Inn and Conference Center in Lewisville (Dallas), Texas.

Microwave Update is the premier microwave conference of the year; initially started by Don Hilliard, WØPW (SK) back in 1985. This is the ideal conference to meet fellow microwave enthusiasts and share ideas and techniques that will help you conquer your next microwave band.

We have a full slate of speakers already set up. If you are interested in speaking, please let us know.

Topics will include small-dish EME, microwave propagation, parabolic-dish feedhorn design and construction, SSPAs, circuit design, latest microwave devices, software defined radios, and digital modes, just to name a few.

We still have several surplus electronics and mechanical places in the DFW area that may be worth a visit on Thursday. A workshop on GNU Radio, led by Tom McDermott, N5EG, is planned for Thursday afternoon. GNU Radio is a development and simulation environment used to create and test software design radio applications. This is a powerful learning tool and GNU Radio can be used to implement working radio applications. Friday morning will be dedicated to "antenna gain." An informal program for the spouses has been planned, and will include local shopping and sightseeing in the Lewisville, Grapevine and greater DFW area on both Friday and Saturday.

Our Saturday night banquet speaker will be Rex Moncur, VK7MO, who has activated over 100 grid squares on 10-GHz EME in both Australia and New Zealand. Rex will show us some of the beautiful places he has visited and talk about his adventures to some of the more remote places down under. This should be a real treat for hams and spouses.

Call for papers: Kent Britain, WA5VJB, will coordinate the publishing of the proceedings by the ARRL. We are always looking for additional papers for the proceedings. You don't have to be a presenter to have your paper published in the proceedings. If you have an article on your latest microwave related project that you would like published, please send your article to Kent, WA5VJB at **wa5vjb@flashnet**.

24th Annual Pacific Northwest VHF-UHF-Microwave Conference

Issaquah, Washington
October 11 – 12, 2019
www.pnwvhfs.org

Join other weak-signal VHF, UHF and Microwave operators for the 25th Annual PNW VHF Society Conference! Details will be added to the website as they become available.

2019 AMSAT Space Symposium, 50th Anniversary

October 18 – 20, 2019
Arlington, Virginia
www.amsat.org

The 2019 AMSAT 50th Anniversary Symposium will take place on October 18 – 20, 2019, at the Hilton Arlington in Arlington, Virginia, next to Washington, DC. Connected to the Ballston Metro Station, the hotel offers easy access to the capital's top tourist destinations, and tours will be available; it's 6 miles from Reagan National Airport. The AMSAT Board of Directors will meet on October 16 – 17, 2019. Information will be posted to the website as it becomes available.

NEW! Take Advantage of a New World of Power and Energy!

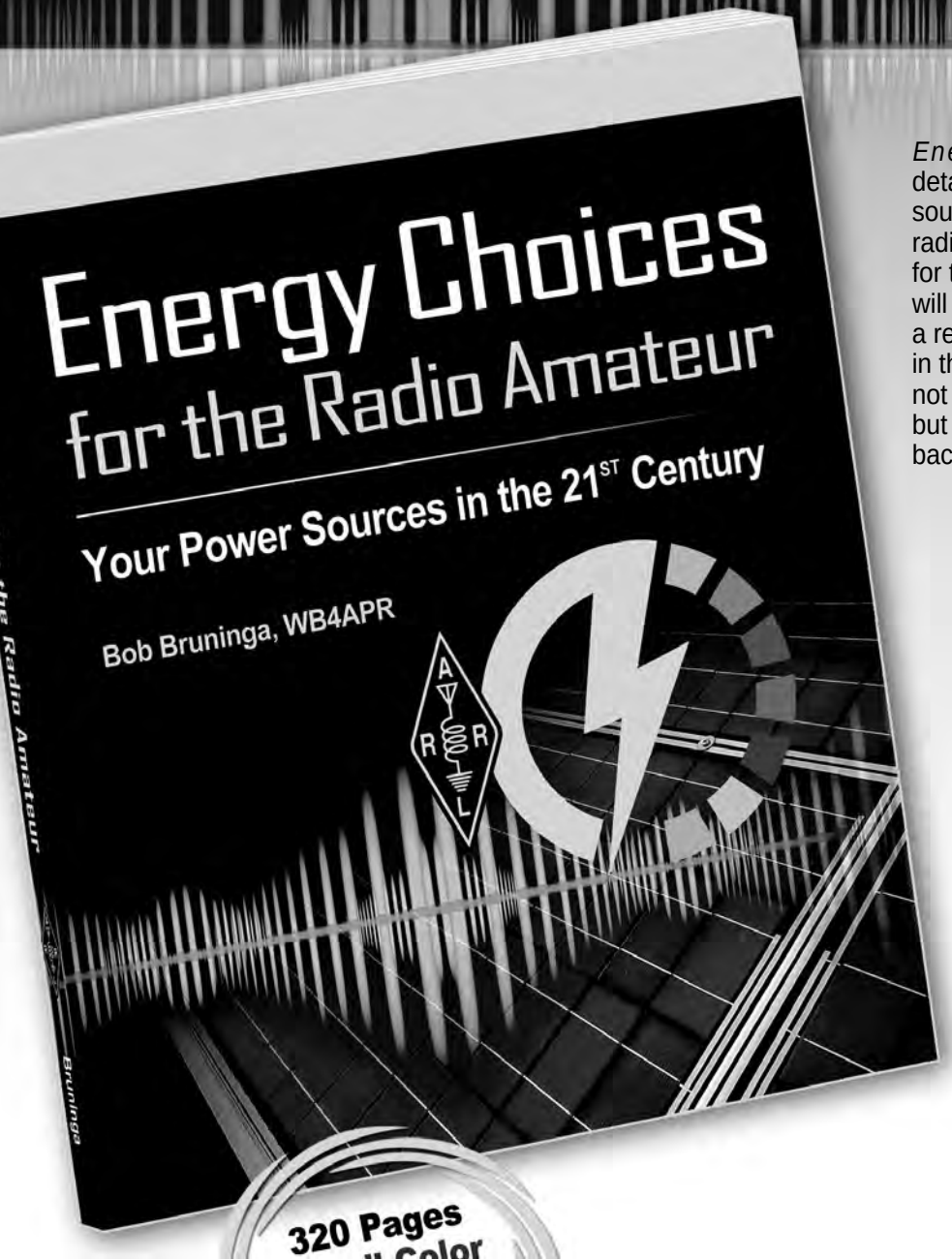

Energy Choices for the Radio Amateur details the author's experiences with new sources of energy. It is intended to help other radio amateurs and DIY hobbyists prepare for the inevitable major energy decisions they will face—choices that can contribute to a reduction in fossil fuel use and save money in the long run. The concepts presented not only satisfy everyday power requirements, but also can help prepare for emergency and backup power at home and in the field.

Chapters include:

- The New World of Everyday Power (DC)
- The Solar Power Revolution
- Choosing Your Home Solar System
- Solar DIY at Home and in the Field
- New Energy Sources of Radio Frequency Interference (RFI)
- Electrification of Transportation
- Electric Vehicle DIY Projects
- Conventional Backup and Emergency Power
- High Voltage DC Emergency and Backup Power
- The Powerwall and Grid Battery Storage for Home
- Life's Major Energy Milestones
- Making the Switch to Clean Renewable Energy
- Amateur Satellites and Thermal Energy Balance
- How Our Energy Use Shapes Our World Today

320 Pages of Full Color Photos and Illustrations!

Energy Choices for the Radio Amateur
by Bob Bruninga, WB4APR
ARRL Item No. 1038
ARRL Member Price! Only $29.95 (retail $34.95)

ARRL The national association for AMATEUR RADIO®

www.arrl.org/shop
Toll-Free US 888-277-5289,
or elsewhere +1-860-594-0355

QEX 4/2019

DX ENGINEERING®

Showroom Staffing Hours:
9 am to 5 pm ET, Monday-Saturday

Ordering (via phone):
8:30 am to midnight ET, Monday-Friday
9 am to 5 pm ET, Weekends

Phone or e-mail Tech Support: 330-572-3200
8:30 am to 7 pm ET, Monday-Friday
9 am to 5 pm ET, Saturday
All Times Eastern I Country Code: +1
DXEngineering@DXEngineering.com

800-777-0703 | DXEngineering.com

Get Ready for Field Day with DX Engineering!

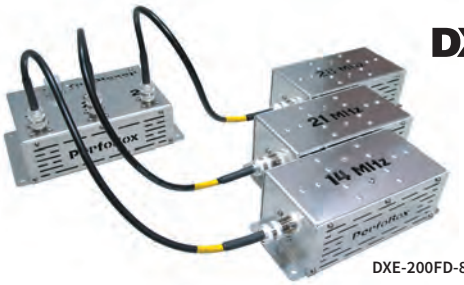

DXE-200FD-8X-P

DX ENGINEERING
LBS LOW BAND SYSTEMS

Field Day Triplexer Combo

We've made it easy to work the 20, 15 and 10 meter bands with three different radios, using just a single tri-band antenna! Our Field Day Triplexer Combo includes Low Band Systems' (LBS) innovative 200W Triplexer (LBS-PB-TP200), LBS 20/15/10M band-pass filters, and coaxial cable jumpers. Eliminate the need (and cost) for extra antennas while enjoying fast setup and worry-free operation without RF interference. The system works with any tri-bander antenna, including DX Engineering's reliable Skyhawk. **For more details, enter "200FD" at DXEngineering.com.**

DXE-200FD-8X-P	**With RG8X cable**	**$649.31**
DXE-200FD-P	**With RG400 cable**	**$743.81**

REU-AA-55ZOOM-BT

REU-AA-230ZOOMBT

RigExpert

Antenna Analyzers

Professional broadcasters, telecommunications engineers and serious Amateur Operators all over the planet trust analyzers from RigExpert. They combine functionality, accuracy, durability, and ease-of-use. These invaluable tools let you test, check, tune, or troubleshoot your antennas and feedlines. Several models are available, with frequency ranges as broad as 0.1-1400 MHz. Two new models (AA-55ZOOM-BT and AA-230ZOOMBT) come with integrated Bluetooth® wireless communications technology.

Enter "Rig Analyzer" at DXEngineering.com for the full story.

GATOR Cases

Gator Equipment Rack Cases

Gator Cases makes virtually indestructible equipment rack cases that are ideal for housing radios, power supplies, antenna tuners and more—whatever you need in your emergency go-kit. Made from sturdy roto-molded or lightweight molded polyethylene, these cases come in rack heights of four or six units and are built tough to secure every element in your portable setup. Racks come in depths of 14.25 or 19 inches.

Enter "Gator" at DXEngineering.com for more information.

DX ENGINEERING
Bushcomm HF Antenna Systems
EAntenna
BUCKMASTER
SB SOTABEAMS
ALPHA DELTA

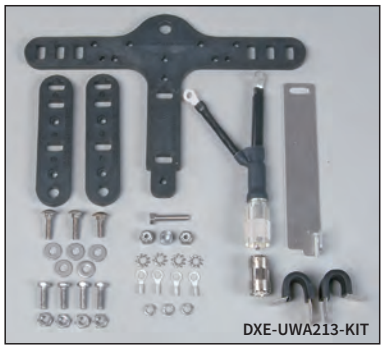

DXE-UWA213-KIT

Wire Antennas

Make us your Field Day source for wire antennas. Choose from DX Engineering's versatile EZ-BUILD UWA Center T and End Insulator Kits that let you build virtually any wire antenna type; fan dipoles from EAntenna that use multiple parallel wires with spacers to allow each band dipole to remain separate; SOTABeams' portable and pre-assembled wire antenna kits; and many more from Alpha Delta, Buckmaster and Bushcomm.

Enter "Wire Antenna" at DXEngineering.com for the complete lineup plus accessories.

YAESU ICOM KENWOOD ALINCO

***Free Standard Shipping for Orders Over $99.** If your order, before tax, is over 99 bucks, then you won't spend a dime on shipping. (Additional special handling fees may be incurred for Hazardous Materials, Truck Freight, International Orders, Next Day Air, Oversize Shipments, etc.).

FAST FREE SHIPPING over $99*

See you at Hamvention®—Building One, Booths 1207-1210 & 1307-1311
Email Support 24/7/365 at DXEngineering@DXEngineering.com

YouTube

A PERFECT PAIR

Combine our manually tuned, ultra-portable yet high performance CrankIR Vertical with the SARK-110 pocket sized antenna analyzer!

CrankIR

A lightweight, high performance, extremely portable vertical antenna rated at 1500 watts key-down with fully manual operation (no electrical power or controller required). An optional portable tunable elevated radial system is available and its patented folded design allows for a 40% reduction in size with only 0.3dB reduction in gain performance when compared to a full sized antenna. With available versions that cover 80m-2m and 40m-2m (and every frequency in between), the CrankIR sets up quickly and provides flexibility to change the bands quickly. This antenna is the choice of amateur radio operators and emergency communications teams world-wide, in both portable and permanent applications. Consider purchasing one of our SARK-110 battery powered pocket sized antenna analyzers for use with the CrankIR – a custom 3D printed mounting bracket is available to secure the SARK-110 to your CrankIR!

SARK-110

The SARK-110 antenna analyzer is a pocket-sized instrument that provides fast and accurate measurement of the vector impedance, VSWR, vector reflection coefficient, return loss and R-L-C. Typical applications include checking and tuning antennas (such as the CrankIR), impedance matching, component test, cable fault location, measuring coaxial cable losses and cutting coaxial cables to precise electrical lengths. The SARK-110 has full vector measurement capability and accurately resolves the resistive, capacitive and inductive components of a load. The SARK-110 is intuitive and easy to use, and utilizes four operating modes: sweep mode, smith chart mode, single frequency mode and frequency domain reflectometer (cable test).

SARK-110

Ask us about our new 3D printed SARK-110 bracket, designed specifically for the CrankIR! *(Prototype holder shown)*

"We introduced the CrankIR to be a world-class portable antenna – little did we know that scores of amateur radio operators would make this their home station antenna as well!"

– John Mertel, WA7IR
CEO SteppIR Communication Systems

steppIR
COMMUNICATION SYSTEMS

FOR DETAILS ON THESE PRODUCTS AND TO ORDER:

www.steppir.com 425-453-1910